Doctoral Dissertations   Graduate School

Fall 1998

Gas-viscous liquid behavior and its implications for pressure-relief design

Ahmad H. Alramadneh
Louisiana Tech University

INFORMATION TO USERS

This manuscript has been reproduced from the microfilm master. UMI films the text directly from the original or copy submitted. Thus, some thesis and dissertation copies are in typewriter face, while others may be from any type of computer printer.

The quality of this reproduction is dependent upon the quality of the copy submitted. Broken or indistinct print, colored or poor quality illustrations and photographs, print bleedthrough, substandard margins, and improper alignment can adversely affect reproduction.

In the unlikely event that the author did not send UMI a complete manuscript and there are missing pages, these will be noted. Also, if unauthorized copyright material had to be removed, a note will indicate the deletion.

Oversize materials (e.g., maps, drawings, charts) are reproduced by sectioning the original, beginning at the upper left-hand corner and continuing from left to right in equal sections with small overlaps. Each original is also photographed in one exposure and is included in reduced form at the back of the book.

Photographs included in the original manuscript have been reproduced xerographically in this copy. Higher quality 6" x 9" black and white photographic prints are available for any photographs or illustrations appearing in this copy for an additional charge. Contact UMI directly to order.

GAS-VISCOUS LIQUID BEHAVIOR AND ITS IMPLICATIONS

FOR PRESSURE-RELIEF

DESIGN

by

Ahmad H. Alramadneh, B.S., M.S.

A Dissertation Presented in Partial Fulfillment
of the Requirements for the Degree
Doctor of Engineering

COLLEGE OF ENGINEERING AND SCIENCE
LOUISIANA TECH UNIVERSITY

November 1998

UMI Number: 9913295

UMI Microform 9913295
Copyright 1999, by UMI Company. All rights reserved.

This microform edition is protected against unauthorized
copying under Title 17, United States Code.

UMI
300 North Zeeb Road
Ann Arbor, MI 48103

LOUISIANA TECH UNIVERSITY
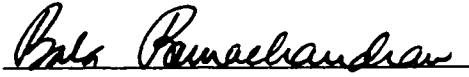
THE GRADUATE SCHOOL

November 2, 1998
_____
Date

We hereby recommend that the thesis prepared under our supervision

by___Ahmad Alramadneh_____

entitled_Gas-Viscous Liquid Behavior and its Implications for Pressure-Relief

_____Design_____

_____
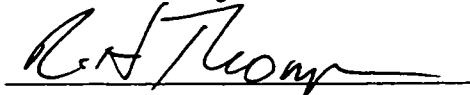
be accepted in partial fulfillment of the requirements for the Degree of

Doctor of Engineering

_____
Supervisor of Thesis Research

_____
Head of Department

___CHEMICAL ENGINEERING_____
Department

Recommendation concurred in:

_____

_____   Advisory Committee

_____

Approved: Approved:

_____   _____
Director of Graduate Studies   Director of the Graduate School

_____
Dean of the College

GS Form 13
2/97

ABSTRACT

The two-phase flow system is a multifaceted engineering task with many industrial applications. The accurate prediction of the behavior of such systems is of special importance.

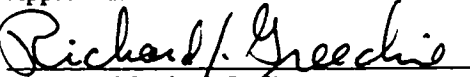This study is directed toward improving and integrating what is known about the gas-viscous liquid flow behavior during vessel depressurization, specifically, visually characterizing the top venting of saturated-viscous fluids. The experimental results are needed to improve the design methodologies for pressure-relief systems.

Lab-scale vessel depressurization experiments with initially saturated fluids were performed. In particular, a problem arose when sodium tetraborate decahydrate solution (model fluid) saturated with carbon dioxide gas is vented from a 5.3-liter vessel.

The test facility has been constructed to permit the visual observation of various influential parameters' effect on depressurization. Parameters examined included the flow behavior response to a change in the fluid properties, the initial liquid fill, the initial pressure, and the vent line diameter. The fluids used were water, foamy fluids, and high viscosity fluids. The resulting level swell, vented mass, and pressure-time profile were recorded and analyzed for each case.

Photographic analysis has been used to examine bubble characteristics and to estimate the bubble size and bubble rise velocity. A high-speed, high-resolution digital camera has been used to capture the depressurization events.

The study presented a useful description for the venting process. The test results are of direct theoretical and practical importance for the design of pressure-relief devices. The study demonstrated that the two-phase flow during the vessel depressurization was strongly influenced by the initial conditions of vessel pressure and liquid level as well as the fluid properties like viscosity and foaming tendency. Further, the study examined the bubble characteristics like bubble size and bubble rise velocity. It was concluded that bubble behavior during depressurization is affected by the system pressure and the fluids physical properties.

DEDICATION

For Abeer and our child to be...

v

TABLE OF CONTENTS

viii

ix

LIST OF TABLES

x

LIST OF FIGURES

xi

ACKNOWELDGMENTS

I would like to begin by expressing my deepest gratitude to my advisor, Dr. Charles M. Sheppard, for his invaluable guidance and his continual support throughout my research. I would like also to thank the members of my advisory committee Dr. Ronald Thompson, Dr. Balachandran Ramachandran, and Dr. Frank Jones for all their guidance and suggestions.

I wish to extend my sincere thanks to the entire faculty and staff in the Chemical Engineering Department at Louisiana Tech University. Special thanks to Dr. Bill Elmore for all the support throughout my studies. Thanks are also due to the Institute for Micro-Manufacturing (IfM) at Louisiana Tech University, especially to Dr. Robert Keynton and Cindy Furlong for their help in using the IfM facilities.

I would like sincerely to thank my family, especially my mother and father, for all the love and continual support. I would like also to thank my wonderful wife Abbora for being the lovely angel in my life through her great communication, understanding, trust, and sacrifices (CUTS).

My gratitude goes to my colleagues in Ruston and Lexington for being the best of friends. Special thanks are due to Mrs. Diane Sheppard and Dr. Ali Darrat for their support and advice.

CHAPTER 1

INTRODUCTION

1.1 Background

Equipment in the chemical process industry often contains hydrocarbons or other flammable chemicals and may involve external heating or energy generation. These chemicals can leak and ignite, or the energy generation can increase beyond design limits. For these reasons, most industrial-process equipment is fitted with pressure-relief devices. This practice dates back to railroad steam locomotives, some of which unfortunately exploded because they were not equipped with pressure-relief devices.

The pressure-relief devices allow the removal of energy from the vessels by either venting of the gas (which contains more energy than liquid) to a safe location or the removal of the liquid, which contributes energy to the system by vaporization or reaction. Thus, the flow behavior of saturated liquids, subjected to a sudden depressurization, is important in safety analysis and other areas. The fluid flow may be all-vapor vented out from the vessel top, all-liquid vented out from the vessel bottom, or both vapor and liquid (i.e., two-phase) from either location. Such a change in the flow of phases requires a different design approach for safety-relief devices.

1.2 Outline of Dissertation Topics

This document is divided into five chapters. In the first chapter, the reader is introduced to the general problem and the main concepts of two-phase flow. The remainder of the current chapter presents the current study practical need and objectives. Also, a description of the two-phase flow behavior with the associated key phenomena is explained.

The second chapter reviews the literature in the area of two-phase flow and briefly discusses the previous investigations in close proximity to the current study. Description of the test facility and the photography equipment is given in chapter three. In addition, it describes the used test fluids and explains a typical test procedure.

Chapter four exhibits the experimental results and the corresponding test analysis. Moreover, the influence of various parameters on the depressurization tests and bubble characteristics is graphically shown. The final chapter presents the study conclusions and lists some recommendations for future work.

1.3 Two-Phase Flow Overview

Gas-liquid flow has been considered the most complex type of the two-phase flow combinations. It combines the compressibility of the gas phase and the deformity of the liquid phase. Two-phase liquid-vapor flow can develop by the addition of energy, a decrease in system pressure, or the mixture of two phases (e.g., air and liquid water) or the combination of the above.

Two-phase, gas-liquid flow can be established by one or the combination of the following methods: mixing of two phases (e.g., air and water) by agitation, introducing

gas bubbles directly into a liquid, adding energy to vaporize a liquid by increasing its temperature, and producing gas through a chemical reaction.

Two-phase, gas-liquid flow is important in a wide range of chemical, petroleum, and industrial applications. For example, steam plants and power production industry. Three other applications for the two-phase flow are (1) Mass transfer in bubble columns, (2) Petroleum vapor-liquid disengagement, and (3) Design of pressure relief device.

In a considerable number of cases, foreseen safety problems during industrial activities may be created by the possibility of a fire, an explosion, a mechanical problem or a toxic release resulting from a runaway reaction. Ultimately, pressure-relief systems are needed to cope effectively with such safety problems or the unlikely events of departure from normal operating conditions. It seems likely that sizing pressure-relief systems is simple and well known for single-phase flow systems. In contrast, the situation is not as well known for high-viscosity, two-phase flow systems. Thus, a precise knowledge of the two-phase flow behavior is essential to design the relief devices as well as to predict the system responses to influential parameters.

1.4 Study Practical Importance

Bubble flow in low-viscosity liquids has been previously researched. However, little work has been done on bubble flow in high-viscosity liquids, in particular the flow of bubbles in pressurized systems. Understanding such a process could improve the design of pressure-relief devices for high-viscosity systems such as polymerization processes.

A major impediment to understand the two-phase flow problem is the lack of experimental results based on visualization of bubble behavior in high-viscosity systems. Visualization is important for the quantification of several bubble characteristics like size, shape, and rise velocity.

The results of this research should improve the modeling of flow and disengagement in high-viscosity systems. The results can also be used to determine conditions under which two-phase flow occurs.

1.5 Research Objectives

This study aims to examine the movement and formation of bubbles in high-viscosity saturated liquids. For this purpose, a sudden depressurization of 5.3-liter vessel containing saturated liquids will be carried out experimentally. Then, depressurization data will be compiled for varying liquid viscosities and a study of vent flow presented.

Closely connected to this goal is the task of predicting the effects of various influential parameters on the venting process. The parameters of fluid viscosity, vessel initial pressure, and initial liquid filling will be varied to determine their effects on the two-phase flow behavior. From the depressurization experiments, the following quantities can be measured and analyzed: the bubble size, the bubble rise velocity, the vessel content swell and the total vented mass.

1.6 Two-Phase Flow Behavior

1.6.1 Description of Venting Process

During the initial stages of the depressurization tests, the pressure inside the vessel continues to rise up to the working test pressure. After the test fluid saturation level is attained, the relief valve opens. The vapor above the liquid surface rapidly empties and the vessel pressure drops. For the two-phase flow venting, the pressure drop rate is expected to be much less than that for all-vapor venting.

After an instant from opening the relief valve, bubbles start to form throughout the bulk of the liquid. As the bubbles continue to form, there is evidence that the vessel pressure increases if the rate of gas bubble generation exceeds the rate of gas discharge.

Upon more bubble formation, the vessel contents swell up to the vessel top. When there is enough swelled liquid level, the vessel contents reach the vessel top and two-phase flow begins through the pressure relief device. It is noticed that if the swell rate is greater than the discharge rate, then some liquid mass will flow back down the vessel wall.

As the bubbles grow in size and some small bubble coalesce to form large bubbles, a void fraction will develop with more bubbles in the vessel top. The vapor fraction leaving the vessel through the pressure-relief device will increase, and the vessel pressure will decrease at a faster rate.

With more venting of both liquid and vapor, the vented mass decreases. At some point, disengagement will occur for bubbles having a positive slip velocity and all-vapor venting will commence. A foam layer may be formed depending on the test fluid properties.

Figure 1 illustrates the vessel-depressurization phenomenon. Upon opening the ball valve, bubbles are generated in the liquid bulk, raising the level of the contents to the vessel top causing two-phase flow through the vent line.
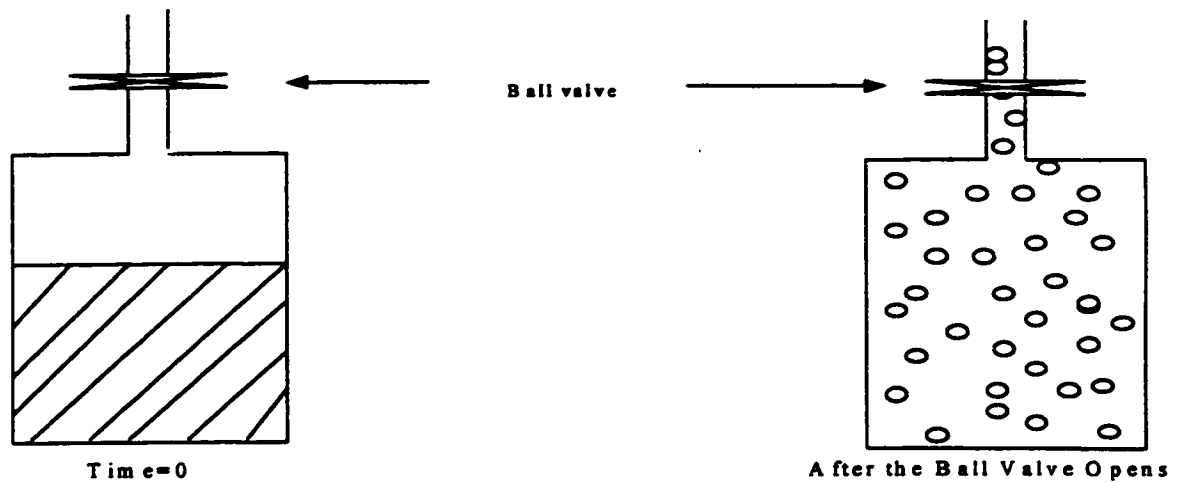
Figure 1   Vessel depressurization phenomenon

1.6.2 Key Phenomena of Two-Phase Flow

It has been found convenient to identify some key phenomena that are expected to be important for the depressurization process. Below each of these phenomena is briefly reviewed.

1.6.2.1 Bubble formation.

Bubble formation requires a nucleus as a void in the liquid-phase volume. A nucleation site is where the bubble forms; it can be in the form of a very small gas bubble or a solid like a dust particle. The vessel wall may also act

as a bubble nucleation site. Usually, bubble nucleation is caused by both the nucleation sites presence and by the supersaturated state of the liquid phase.

Very early, Kenrick et al. [1924] explained that bubbles are originated from a spherical particulate acting as a nucleus. The diameter of such nucleus calculated to be at most 0.23 micron. Many models have been forwarded for the bubble formation; Griffith [1960] conducted one such attempt. However, such models are limited in scope because of the large number of variables associated with the bubble formation and nucleation, which greatly complicates such efforts.

Attar [1978] reported that rough surfaces determine the critical nucleation radius and thus significantly accelerate the rate of nucleation. Further, he pointed that bubble nuclei are in the order of 0.01 micron, and developed bubbles can be examined by microscopy once they reached size of 1 micron. Gas bubbles trapped in cavities may also act as a continuous nucleus and may enhance bubble formation.

During depressurization of liquids from a vessel, part of the overall gas bubble generation occurs at the vessel walls, including the bottom. Boesmans and Berghmans [1995] developed a model for the bubble generation, which includes the effect of bubble generation at the walls.

1.6.2.2 Bubble growth. The growth of bubble nuclei is limited by the fluid properties such as the density and the viscosity. According to the nucleation theory, section 2.3, the nuclei grow in size due to fluctuation in liquid density. Bubbles may grow by coalescing through additional mass or by reduction of pressure and density. However, bubble growth via density reduction is typically small compared to the addition of mass. For coalescing bubbles to grow, they must overcome the liquid

surface tension. Street et al. [1971] studied the dynamics of bubble growth in viscous, non-Newtonian fluids. They modeled the growth of an individual bubble in the liquid bulk. The model describes the growth process quite well. Amon and Denson [1984] proposed a thin shell of fluid surrounding each bubble, which limits the growth of bubbles depending on force balance (surface tension and pressure) between the shell.

1.6.2.3 Bubble rise velocity.

It is the velocity at which individual bubble rises in the bulk of the fluid. Bubble rise velocity depends on the fluid properties of density, viscosity, and surface tension. Figure 2 shows some of the bubble characteristics. Fisher et al. [1992] reported that bubbles are rising through the liquid with a velocity dependent on the buoyancy and the liquid surface tension. However, the viscosity and the foamy nature of the test fluid retard the rise velocity.

In determining the bubble rise velocity, the wall effects and the adjacent bubble effect is neglected or eliminated. According to Bell and Morris et al. [1992] and Bell et al., [1993] the micro- bubbles are assumed to have a small slip velocity compared to the macro-bubbles, which have a larger slip velocity. Wallis [1969] pointed that rise velocity is a function of bubble size for lower-diameter bubbles and may approach a constant value as the bubble grows.

Manjunath and Chabra [1992] studied mono-sized spherical gas bubbles traveling in a liquid swarm with Reynolds number less than 50. They investigated a range of gas holdup values and calculated the drag coefficient. They also outlined a method to estimate the free rise velocity of bubble swarms for a clean gas–liquid interface.

Using the hydrodynamic theory of waves, Mendelson [1967] has proposed an early model to calculate the terminal rise velocity in purified systems (pure liquids) for bubbles of intermediate to large size. More recent, Fan and Tsuchiya [1990] developed a general model from which they predicted the terminal velocity of bubbles. The model is applicable to both viscous and distorted flow regimes.
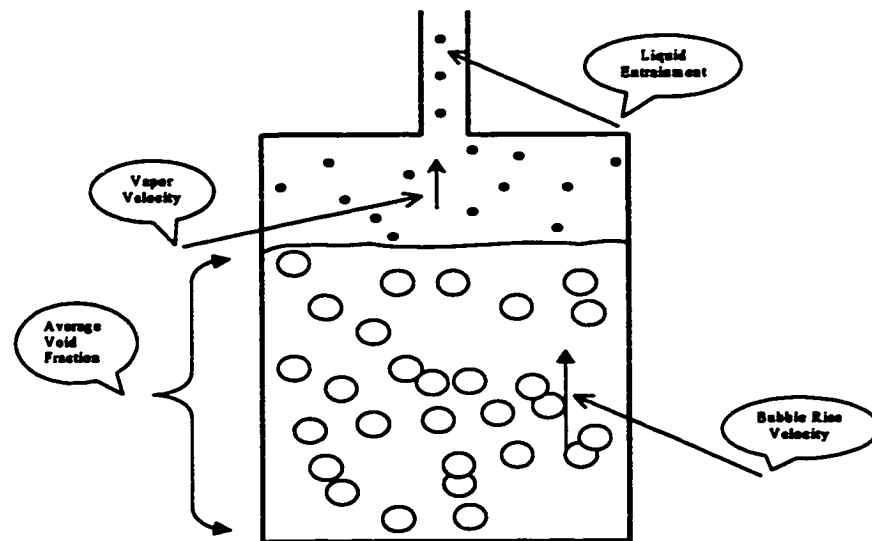
Figure 2 Bubble characteristics

1.6.2.4 Swell level. During the depressurization of saturated liquids, vessel contents flashes result in two-phase flow. Liquid surface level will rise if the rate of vapor generation is greater than the rate of vapor escape from the liquid. In other words, liquid-vapor interface can rise to the vessel top if enough bubbles have

accumulated in the vessel. If the initial liquid level is low enough, the level of the two-phase mixture in the vessel decreases and all vapor flow occurs.

Thus, an accurate knowledge of the liquid swell rate will help to predict whether the two-phase flow mixture will reach the vessel top, and hence to account for the two-phase flow venting in the pressure-relief device design. Generally, swell level increases with increasing bubble formation rate, and it is greatly influenced by the fluid properties such as viscosity and foaming tendency.

The liquid swell level can be calculated based on the vapor generation rate and the slip velocity. Sheppard [1992] illustrated such analysis for churn turbulent regime, in which the slip velocity has a single value independent of bubble diameter. For viscous flow, two bubble sizes (micro and macro) have been postulated with their associated slip velocities. Using the distribution ratio between the bubble sizes, the swell level can also be calculated. To include the effect of vapor generation from the vessel bottom (resulting from heterogeneous nucleation) Boesmans and Berghmans [1995] showed a theoretical procedure to estimate the level swell. This approach leads to better and safer results.

1.6.2.5 Vented mass. Various parameters including the nature of the vessel inventory (viscous/foamy) and the test working conditions (initial filling/initial pressure) may influence the amount of vented mass. Fisher et al. (1992) showed that several two–phase flow models exist for the determination of the discharged fluid mass through the vent line at sonic velocity. Among these models are the homogeneous equilibrium flow model and the homogeneous non-equilibrium flow model. From such models, the flow velocity profile can be depicted and analyzed.

It is expected that liquid will flow back down the vessel wall if the mass discharge through the vent is less than the mass flow inside the vessel. This situation is also normal in bubble columns.

1.6.3 Flow Configurations

From visual observations, many flow regimes have been defined in the literature. Hetsroni [1982] has identified the following flow regimes for vertical flow in tubes.

1. Bubbly flow. A dispersion of bubbles flows within a continuous liquid phase.

2. Slug or blug flow. At higher gas flow, bubble coalescence occurs and large diameter bubbles approach that of the tube are formed, separated by dispersions of smaller bubbles.

3. Churn flow. With increasing flow velocity, a breakdown of bubbles leads to an unstable liquid flow of an oscillatory motion upward and downward the tube. Both distinct and large bubbles are present.

4. Annular flow. Liquid film flows down the tube walls while the gas phase flows in the tube center.

5. Wispy annular flow. With higher liquid flow rates, the bubble concentration in the gas phase increases. Ultimately, bubbles in the center coalescence forming large lumps or streaks.

Two flow regimes are of special interest to our study, the bubble flow and the churn turbulent. The bubbly flow configuration is the easiest flow regime to visually observe; the gas bubbles are distributed in the liquid phase with rising velocity of same order. Figure 3 illustrates the main bubble features of each flow pattern.

| Bubbly flow | Blug flow | Churn flow | Annular flow | Wispy Flow |
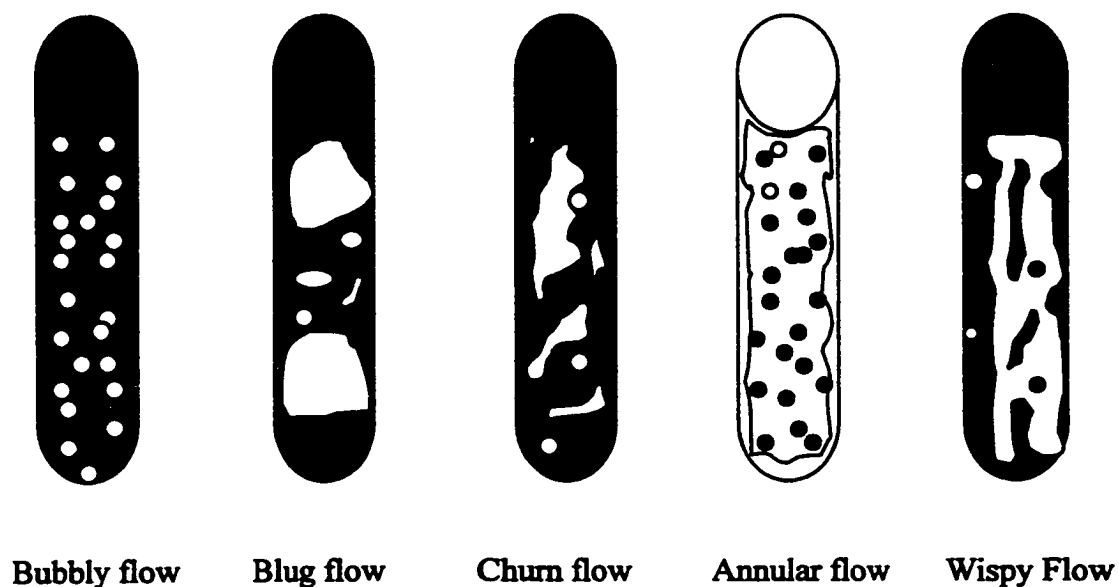
Figure 3 Flow patterns in vertical flow

1.6.4 Pressure Relief Valves

Pressure vessels are usually filled with fluids with some vapor space above the liquid level to account for the liquids thermal expansion. Pressure valves are designed to vent vapor, and consequently they are located at the vessel top (i.e., above the liquid level).

The size of the valve is influenced by the phase nature of the vent flow. Depending on the swell level inside the vessel, the initial liquid filling, and vessel geometry the vent flow can be one or two phases.

Normally, pressure valves are exposed to a variety of different flow conditions. Of particular importance is whether the valve is designed for single or two-phase

(vapor-liquid) flow. The pressure relief valve capacity is greatly reduced when two-phase flow occurs.

CHAPTER 2

LITERATURE REVIEW

Despite the complexities of high-viscosity, two-phase flow systems, a considerable amount of published material is available in the literature. Many studies of both theoretical and experimental origins have been successful in investigating many aspects of the two-phase flow problem. These efforts will be briefly discussed below.

2.1 Background

The need to account for the two-phase flow in relief-system design was recognized by Boyle and Huff two decades ago. Boyle [1967] appears to be the first to develop a procedure for sizing relief devices for two-phase flow venting, while Huff [1973] pioneered a comprehensive method for sizing two-phase, emergency-relief devices.

For long time, researchers and engineering groups have recognized the need for safety and adherence to the regulations in the chemical industry. For this reason, the design Institute for Emergency Relief Systems, known as DIERS, was formed in the mid-1970s to develop methods for designing emergency-relief systems. The group carried out a series of integral blow-down and runaway-reaction experiments for two-phase, vapor-liquid flashing flow. The group experimental work also included depressurization tests from well-instrumented small and large vessels.

14

DIERS' experimental results were simulated into a computer program called Systems Analysis for Integral Relief Evaluation, SAFIRE. The program has the capability to describe the multiphase dynamics of two-phase flow, emergency-relief systems. Other contributions of DIERS resulted in a new design methodology to determine the onset and disengagement dynamics of two-phase flow systems. Another significant finding of DIERS' program is the ease with which two-phase flow can occur during an emergency-relief situation.

2.2 General Overview

Compared to single-phase flow, two-phase (liquid-vapor) discharges are complicated more by the flashing behavior of the two phases. An accurate knowledge of such flow is essential for the equipment design of many chemical and industrial applications. Due to this need, the phenomenon of two-phase flow has been extensively studied in recent decades. The studies of Fauske & Associates, Inc. [1981] are perhaps the best known of these analyses.

Finke [1990] studied the top venting of various test-fluids (including water and high viscosity fluids) from a 400mm vessel to a 20mm tube. Further, he studied the level swell of fluids when air is bubbled through a liquid under atmospheric conditions. The influence of liquid viscosity and of vessel diameter was also examined and a relationship between vessel and vent line void fraction was made.

Based on top venting of high viscosity fluids, Morris et al. [1992] proposed a simple design method for estimating the initial two-phase discharge rates. In addition, they described a practical method for sizing pressure-relieve devices. Friedal and Purps [1984] carried out depressurization experiments using R12 saturated-refrigerant as the

model fluid. They concluded that vertical distribution of the void fraction across the vessel height depends on the initial liquid level, the relief cross section area, the initial pressure, and the initial degassing of the liquid pool.

The work of Skouloudis and Kottowski [1990] aimed at understanding the hydrodynamic phenomenon associated with the top and bottom depressurization of vessels. They employed comparative tests of five depressurization experiments in vessels containing water under saturation conditions. They also examined the liquid swell level and the vessel void fraction. In a later study, Skouloudis and Kottowski [1991] also analyzed a nine depressurization experiment for vessels containing water, freon-114, and high-viscosity fluids. Their study provided information about the dependence of the depressurization process on the initial conditions, the vessel size, and the position of the vent line. The differences between venting into the atmosphere and venting into a collecting tank have been also examined.

Fauske & Associates, Inc. [1989] studied the effect of vent line length-to-diameter ratio on the discharge flow rate of some fluids. They also included a discussion on scale-up methods of the experimental results.

More recently, Sheppard and Morris [1994] discussed the relevance of disengagement and void fraction to pressure relief system designs. For venting of a vessel containing a viscous fluid, a simple model has been proposed to describe the system behavior. The model is based on certain assumptions including zero micro-bubble slip velocity. To solve the model, they proposed two types of experiments to measure and correlate the macro-bubble slip velocity and the critical void fraction at different viscosities. The present study is an attempt to conduct such experiments.

As it can be seen, the importance of accurately predicting the size of two-phase process equipment has been recognized by a large number of analytical and experimental studies. Ultimately, such knowledge can reduce the cost of over-design and avoid the problems resulting from under-design of process equipment.

2.3 Nucleation Theory

A surface is where an abrupt change in the properties of the material occurs. Due to the presence of such surfaces, nucleation can be classified as homogeneous or heterogeneous. Homogeneous nucleation occurs throughout the bulk of the liquid solution where surfaces have no or little effect on the system. In this regard, Cole [1974] has reviewed various aspects of the nucleation theory. Blander and Katz [1975] also studied the theoretical and experimental aspects of homogeneous and heterogeneous nucleation including the hydrodynamic and diffusion constrains.

Depressurization of supersaturated solutions usually produces a fine dispersion of bubble throughout the volume of the liquid. It is expected that such small bubbles are being formed homogeneously. Evidence to support such a premise has been reported by Morris et al. [1992] and Bell et al. [1993]. They performed depressurization tests and observed the formation of cloud of bubbles in the bulk of the liquid.

2.4 Bubble Coalescence

At a certain void fraction, large bubbles begin to form via coalescing of small bubbles. Bubble coalescence occurs in three steps: (1) Two bubbles collide trapping a thin liquid film between them (2) The liquid film drains to a certain critical thickness

and (3) The liquid film collapses due to instability mechanism resulting in bubble coalescence.

The rate of bubble coalescence is important in many applications, including the stability of foams when venting foamy fluids. Allen et al. [1961] studied the effect of some physical properties like surface tension on the rate of bubble coalescence. They suggested that the rate of coalescence is directly affected by the concentration of surfactants. In this connection, Sagert and Quinn [1978] have conducted a similar study. The results showed that for fluids with a large surface tension, the drainage rate of the thin liquid film around the bubble is the slowest. However, when the surface tension and surface viscosity is minimal, the thinning rate is the fastest and bubbles coalesce more easily.

Dongming [1996] has developed a model for the dynamics of film thinning which predicts the coalescence time. He further investigated the effects of mass transfer and fluid physical properties on the film drainage rate.

2.5 Depressurization of High-Viscosity Fluids

An important problem associated with two-phase flow is incurred in accounting for high-viscosity systems. This problem has received considerable attention in recent years. Bell [1994] studied the influence of liquid viscosity on the depressurization of non-reacting fluids and described how the liquid viscosity affects the vessel flow pattern. The results from both a small- and large-scale experiment are used to study and model the physics involved in the depressurization of high-viscosity, non-reacting fluids.

In an earlier study, Bell et al. [1993] presented experimental data for top venting of high-viscosity fluids; they examined the influence of the initial liquid filling and the fluid viscosity on the vent line void fraction.

Bell and Morris [1992] also performed experiments in a small glass vessel to study the venting behavior of foams and high-viscosity fluids. Results based on a high-speed video recording showed that differences in venting characteristics such as the pressure history and the vented mass are due to differences in the flow regimes.

Fauski [1987] reported that viscosity was found to have a drastic effect on maximum flux during DIERS program on investigating the depressurization of different viscosity fluids.

2.6 Bubble Size

Factors conceivably affecting the bubble size are the test fluid's physical properties of density, surface tension, and viscosity. System pressure also may influence the bubble size. However, the mechanism of how the pressure affects the bubble size is not fully understood. In regard to this question, Jiang et al. [1995] employed Particle Image Velocimetry (PIV) to characterize the bubble flow in a gas-liquid bubble column operated at maximum pressure of 21 MPa. The study explained how the pressure affects the bubble size and its distribution. They also reported an increase in the gas holdup and a decrease in the bubble size with increasing pressure. In the vicinity of such findings, Idogawa et al. [1986] reported similar results.

Reilly et al. [1994] studied the role of gas phase momentum in determining the gas holdup, he attributed the pressure effect on the bubble size to an increase in the gas momentum. In a similar study, Jiang et al. [1992] explained the pressure effect by the

reduction in interfacial tension, which affects the liquid film thinning and the bubble instability.

Akita and Yoshida [1974] reported experimental results on average bubble size as a function of liquid properties. The photographic method was used to determine the size of oxygen or air bubbles in a bubble column. They also proposed dimensionless correlation for the average bubble size.

Fan and Tsuchiya [1990] noticed that the bubble flattens while moving in the direction of its motion, and its size increases due to the positive difference between the pressure forces inside the bubble and the surface tension force. When the bubble size is small, surface tension forces controls and the bubble shape is spherical. During depressurization both stable and unstable bubbles may be formed. Blander and Katz [1975] reported that for a spherical bubble to be stable, it must exceed a certain critical radius (r_c). Bubbles smaller than r_c tend to collapse and bubbles larger than r_c tend to continue to grow.

2.7 Bubble Rise Velocity

It is expected that bubble rise velocity experiments will provide data on bubble characteristics as a function of bubble size and fluid properties. Bubble rise velocity is often required to measure the bubble drift velocity and hence the vessel void-fraction.

Many correlations are present in the literature to account for the bubble rise velocity in different flow regimes. Peebles and Garbar [1953] studied the dependence of bubble rise velocity on the bubble size in different fluids. Haberman and Morton [1953] have studied the shape and the rise velocity in various liquids and have shown that impurities in the liquid phase decrease the rise velocity. Wallis [1969] also

reported that bubble rise velocity depends on the liquid viscosity and flow pattern at low Reynolds numbers.

Marrucci [1965] proposed a model relating the velocity of rise of a swarm of spherical bubbles to the velocity of a single bubble. Mendelson [1967] related the rise velocity of bubbles to the hydrodynamic theory of waves. He proposed a model to calculate the terminal rise velocity in purified systems for bubbles of intermediate to large size. In a related study, Fan and Tsuchyia [1990] developed a general model for determining the bubbles rise velocity. The model is applicable to both the viscous and distorted flow regimes.

Vassallo et al. [1995] used a photographic technique to obtain the terminal velocity and shape of isolated freon-114 bubbles in a rectangular test section. Bell et al. [1992] reported a small slip velocity for the generated micro-bubbles and a much larger velocity for the macro-bubbles.

2.8 Summary

As evidenced by the preceding discussion, it is obvious that the gas-viscous liquid depressurization has received an extensive study. The investigations satisfactorily explained many aspects of the problem. However, it is worth pointing out that several other aspects of the overall problem remain in question.

It may also be noted that many investigators have dealt primarily with mixtures of steam and water to represent the two-phase flow systems. On the other hand, the chemical industries often use a mixture of various components other than the steam-water mixtures. For this reason, some of the existing literature is of a limited value for many industrial applications.

In light of our knowledge, most previous studies are not entirely satisfactory for predicting system response during depressurization. More focus and attention is needed to visualize vessel depressurization process of high-viscosity, saturated-fluids. This study, by contrast, will endeavor to gain an intuitive understanding of high-viscosity venting as well as to visually simulate the behavior of a saturated system during a two-phase flow discharge.

CHAPTER 3

METHODOLOGY

3.1 Description of the Depressurization Facility

The depressurization facility is schematically depicted in Figure 4. Listed below is a description of the experimental set-up.

3.1.1 Test Vessel

The vessel comprises a vertical cylindrical sleeve of transparent clear acrylic martial, which permits the visual observation, and the photographic documentation of observed events. The vessel is closed at both ends by 1-inch thick flanges and sealed by an -O- ring rubber band and 8 restraining bolts. The vessel is 14 inches in height, 5.5 inches in diameter, and has a measured internal volume of 5.3 liter.

The vessel was pressure-tested up to 120 psi; this will be the maximum operating pressure for the vessel. The pressure is given by a pressure gauge mounted at the vessel top. The gage is supplied by Harris Calorific Co. and has a pressure range of 0-200 psig.

23

1. 1/4 inch Pressure Relief Valve. **2.** Pressure Gage.
3. 1/4 inch Quick Acting Ball Valve. **4.** Pressure Regulator.
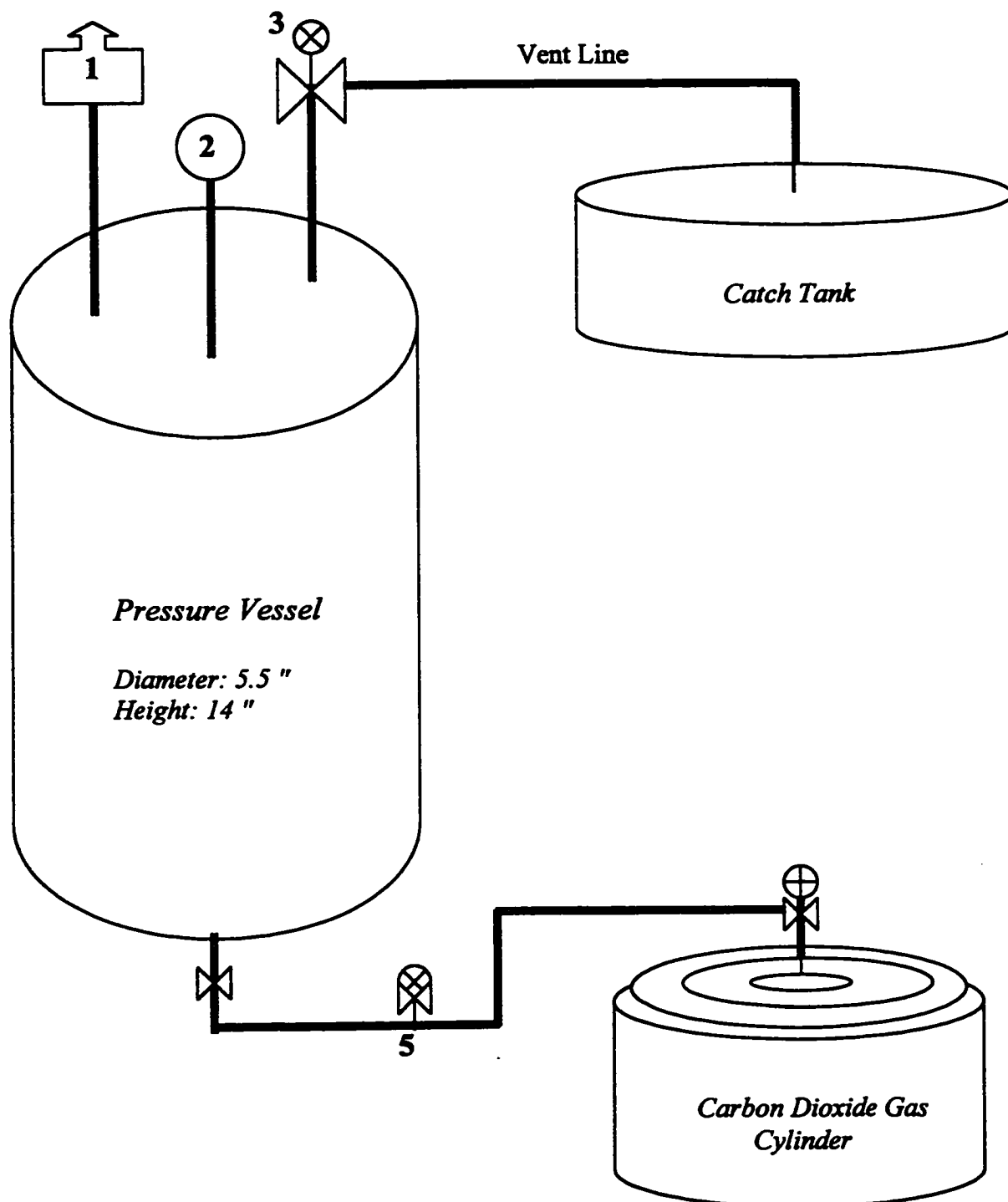
Figure 4 Depressurization facility

3.1.2 Pressure-Relief Valve

For emergency venting, the vessel is equipped with a 1/4-inch PVC pressure relief valve supplied by Plastic-O-Matic Valves Inc. The relief valve has a 1.013-1033 kPa variable setting pressure range and opens once the vessel pressure exceeds a certain set value. The relief valve (located in the centerline of the vessel) protects the vessel against over-pressures by opening up a relief path for the vessel contents to the catch tank.

3.1.3 Ball Valve

The vessel is closed by a 1/4-inch quick-opening ball valve supplied by Chemtrol. The valve is made of PVC operating at a maximum pressure of 150 psig (at 100 °F) and gives an obstruction free flow with rapid opening speed estimated at 0.4 seconds. Depressurization is initiated by opening the valve installed at the vessel top. The pressure valve can create a pressure drop inside the vessel and significantly influence the discharge rate (maximum 5 ft^3/sec). For this reason, the valve characteristics are important in modeling the vessel behavior.

3.1.4 Vent Line

Two vent lines (4-mm and 6.35-mm in diameter) will be used to study the vent line size influence on the fluid flow behavior. Changing the cross sectional area of the vent line is expected to influence the rate of mass discharge from the vessel. The two vent lines (0.7 m in length) are attached to the vessel top.

3.1.5 Collecting Tank

A 25-liter tank connected to the vent line outlet is used to collect the discharged test fluids.

3.2 Fluid Properties

Viscosity and surface tension are two crucial fluid properties. They are expected to influence the two-phase flow system behavior. Owing to the basis of the relative value of these properties, the fluid can be classified as low viscosity or high viscosity and as foamy or non-foamy. Water, for example, shows low viscosity and non-foamy fluid behavior.

3.2.1 Viscosity

Viscosity is perhaps the most important physical property that characterizes the flow resistance of fluids. It measures the internal friction of a given fluid. The movement of fluid layers relative to each other is called shear. It is believed that shear stress introduces deformation that sets up the internal resistance.

Newton used this idea to define the viscosity by considering two parallel fluid layers of equal area A, separated by a distance Y. At time zero, the lower plate is set in motion at constant velocity V. The force F per unit area required maintaining the motion of the lower plate (at steady state) is proportional to the velocity decrease in the distance Y. Hence, this force F may be expressed as follows:

$$(F/A) = \mu \, (V/Y)$$

The above formula represents Newton's equation of viscosity. It states that the shear stress is proportional to the local velocity gradient. The velocity gradient describes the difference in layer velocity with respect to the distance Y and is called the

shear rate. The force per unit area (F/A) is referred to as shear stress. The constant of proportionality (μ) is called the viscosity.

As already known, the fluids that do obey Newton's law are referred to as Newtonian fluids. Laminar flow is expected to obey Newton's equation of viscosity. The unit of viscosity in the SI system is given by N.s/m^2 or Pa.s (mPa.s equals 10^{-3} Pa.s). In cgs system, viscosity is given by (g cm^{-1} sec^{-1}) and called poise (P). centipoise (cP) is also in common use (1 cP=0.01 P).

3.2.2 Surface Tension

Surface tension is defined as the tensile strength of the liquid surface film computed per unit length and has been given the symbol (σ). Surface tension is expressed in SI units as (N/m). Surface tension can be reduced by addition of certain chemicals like soap and alcohol.

Many methods are available to measure the surface tension. Adamson [1982] reviewed various experimental and analytical methods to measure the surface tension. Capillary method is considered the most accurate; it is based on measuring the height (h) to which a liquid rises in a capillary tube and the contact angel (θ) between the fluid surface and the tube wall. For a circular tube with a diameter d, the surface tension σ is given by the following equation:

$$\sigma = h \, \rho \, g \, d \, / \, 4COS \, \theta$$

Where ρ is the fluid density and d is the tube diameter. In this study, the Capillary method will be used to measure the surface tension of test fluids.

A widely used method to measure surface tension is called the Ring method. A device called Interfacial Tensiometer is used to measure the force required to pull a ring or a loop wire from or through the liquid interface.

3.3 Test Fluids

Three test fluids were used for the current study. They are water, high-viscosity sodium tetraborate decahydrate solution, and (409 formula) foamy solution.

3.3.1 Water

Distilled water was used in order to minimize the effects of dissolved gases on the test results and to maintain consistency in test fluid conditions.

3.3.2 High-Viscosity Fluids

For the use of this study, high-viscosity fluids were made by dissolving carboxymethylcellulose (CMC) in water. CMC is a white powder supplied by Aldreich Chemical, Inc., and has the advantage of increasing the fluid viscosity with little effect on other physical properties. According to the manufacturer specifications, a water solution of 1% CMC by weight gives a viscosity of 4.5 Pa.s. A maximum viscosity of 62 mPa.s was used in the current study. The fluids were found to be Newtonian, since a constant measurement of viscosity was obtained under different shear rate. Viscosity measurements were made (under ambient conditions) using a Cannon-Fenske Routine Viscometer supplied by Industrial Research Glassware Ltd.

3.3.3 Foamy Fluids

Foam is defined as a group of bubbles separated from one another by a thin film, formed with a finite static life when bubbles rise to the liquid surface. The foamy nature of test fluids is expected to significantly influence the characteristics of the two-phase flow.

The addition of small amount of household detergent (Cleaner) supplied by Clorox leads to the formation of foams above the liquid surface. It was experimentally observed that a small amount of the detergent (0.5% by volume) was sufficient to significantly produce foams with a reduced surface tension.

3.3.4 Carbon Dioxide Gas

CO_2 gas is readily available, inexpensive, odorless moderately water soluble, and nonflammable with a few toxicity dangers. Red Ball Oxygen supplied the CO_2 gas through a 2000 psig cylinder. A two-stage regulator, regulates the inlet gas pressure and two gate valves control the gas flow rate.

3.4 Super-saturation of Test Fluids

In the present study, carbon dioxide gas was used as the gas phase. The degree of carbon dioxide saturation in the test fluid is a function of many parameters including mixing time, solution concentration, vessel pressure, and solution temperature.

The super-saturation of carbon dioxide in beverages is of special importance to the bottling industry. In agitated solutions of gases, the rate of super-saturation is directly proportional to the concentration of the gas in the solution and also directly proportional to the saturation pressure.

In general, gas solubility can be expressed by many formulas including Bunsen absorption coefficient (α) which is defined as the ratio of the volume of gas which passes into solution (through unit area in unit time) to the volume of gas which is similarly passed out. Appendix B gives the absorption coefficient (α) of some organic compounds.

For the depressurization experiments, an aqueous solution of 25 g/l - sodium tetraborate decahydrate ($Na_2B_4O_7.10H_2O$) supplied by Aldreich Chemical Company, Inc., was used as the test fluid. Solubility of carbon dioxide is high in sodium tetraborate decahydrate. As can been seen from the solubility data given in appendix B, carbon dioxide solubility in solutions of sodium tetraborate decahydrate is six times as soluble in water. Twenty percent of the test fluid will be isopropyl alcohol additive to enhance the carbon dioxide solubility. In general, alcohol solutions are good solvents for carbon dioxide gas. See Appendix B for alcohol solubility data.

Saturated test fluids were prepared by thoroughly mixing the test fluids with carbon dioxide gas under pressure. Mixing is accomplished via shaking of the entire vessel. During the course of this research, a maximum allowable working pressure of 8 bars was employed. Saturation point was reached when no further carbon dioxide gas can dissolve into the solution; i.e. the maximum solubility was reached.

3.5 Photography

The Quantix High Charge-Coupled Device (HCCD) camera, supplied by Photometrics Co., was used to obtain bubble images and to record the depressurization event. Quantix is a versatile imaging system that combines fast readout rates (5 million

pixels per second) with low read noise. The camera digitization and computer interface has been consolidated within one compact camera head.

Quantix was easily connected to a 50-mm auto-shut lenses supplied by Olympus OM-System. It was possible to focus at a distance of 0.5-2 meters from the vessel. The illumination was a conventional white light. Sheets of white papers were placed in front of the light to minimize the light reflection. See Appendix A for detailed Quantix CCD camera specifications.

For the purpose of studying bubble properties, the camera images were transferred to a personal computer where bubble size and shape were obtained through image analysis software called V for Windows. This software is an advanced image enhancement and analysis package that runs under Microsoft Windows. V for windows contains hundreds of operations for image processing, enhancement and analysis. A part of the V for Windows powerful operations is the contrast and color processing, the counting and object shape analysis, and the geometric operations.

3.6 Test Procedure

A typical experimental test sequence consists of the following steps:

1. Care is taken to ensure that the entire vessel system is clean, all interior surfaces of the vessel are cleaned and flushed before each test. The vessel is carefully checked out for possible leaks by employing a soap solution,.

2. The test fluids are prepared according to the required properties like the viscosity and the concentration.

3. The vessel is filled with test fluids up to the required initial filling height.

4. Carbon dioxide gas is introduced into the vessel bottom directly to be mixed with the test fluids. Meanwhile, the ball valve at the vessel top is left open for a few minutes to let the carbon dioxide gas expel any air left inside the vessel. The vessel is then sealed to the atmosphere so the pressure builds up to the desired initial pressure.

5. The vessel contents are agitated to enhance the carbon dioxide solubility in the test solution, and the mixing continues for about ten minutes to ensure carbon dioxide saturation conditions under the test pressure.

6. Depressurization is initiated by suddenly opening the quick-acting ball valve. The high-resolution digital camera is started to record the blow down events. The discharged solution is disposed to the adjacent collecting tank.

7. Results of vessel depressurization are analyzed and discussed based on the photographic observations as well as other quantitative measurements

8. The vessel is finally drained out to be ready for the next test. In each experimental run, a fresh test fluid is used to avoid the impurity problem that could affect the results.

Experimental results of various depressurization tests will be presented and analyzed in chapter four.

3.7 Safety Considerations

Special precautions are necessary to ensure safety during the depressurization tests. Support frames and couplings for the vessel were provided to restrict the vessel movements and to suppress vibrations resulting from the action of the quick opining valve and fluid flashing.

To ensure a safe work environment, isopropyl alcohol was chosen because of its low health hazards and the insignificant level of reactivity. However, caution must be exercised in handling all test fluids during experimentation.

CHAPTER 4

EXPERIMENTAL RESULTS AND DISCUSSION

4.1 Overview

In the current study, two types of information are essential in characterizing the fluid flow patterns during depressurization, the pressure-time profile and the total vented mass. Important indicators of change such as the initial liquid filling and the initial pressure in the vessel were varied. Then the corresponding changes in the vented mass and the pressure-time profile were recorded. The pressure history inside the vessel during the depressurization is important in understanding the physical processes involved. The vented mass indicates the average mass flow rate through the vent line, and such information is important in designing the relief valve.

Typically, during two-phase pressure relief, process variables and fluids' physical properties are changing. However, throughout the depressurization experiments of this study, two assumptions have been made: the vessel was assumed to remain at constant room temperature, and test fluids density is also assumed constant.

For the depressurization tests, a base case of 80-psi pressure and 70% initial liquid filling is considered, and other variables will be stated with each test.

For simplicity and convenience, the test fluids used in this study will be referred to as follows; sodium tetra borate decahydrate (SB) and isopropyl alcohol (IA).

34

4.2 Effects of Influential Parameters on Depressurization

Investigations were made for the influence of the initial liquid level, the initial pressure, the vent line diameter, and the liquid viscosity on the depressurization process. The following sections will address the experimental observations for each case.

4.2.1 Influence of Initial Liquid Filling

Five tests were performed to determine the influence of the initial liquid filling on the depressurization of SB/IA mixture solution. The initial liquid fillings chosen were 50, 60, 70, 80, and 90% of the vessel volume, corresponding to 2.75, 3.3, 3.85, 4.4, and 4.95 liters respectively. Initial pressure of 80 psi was chosen as the base case. The working fluid, the vent line size, and the starting conditions are summarized in Table 1.

Table 1 Starting conditions for the initial liquid filling effect on the vented mass

Test Fluid	SB/IA
Initial Pressure	80 psi
Initial Filling	50, 60, 70, 80, and 90%
Viscosity	1 mPa.s
Vent Diameter	6.35 mm

The measured vented mass (collected at the catch tank) for different initial fillings are presented in Figure 5. The vented mass has been expressed as a volume percentage of the initial mass inventories.

As can be seen, the discharged mass increases with increasing the vessel initial liquid filling. For higher initial liquid filling, a larger amount of bubbles has been generated, causing higher void fraction in the liquid bulk so that the liquid surface is nearer to the vessel top, giving more of two-phase venting. In other words, the mass of vapor generated through depressurization is a function of the initial filling (i.e., mass of liquid in the vessel). Thus, the amount of liquid entertained in the discharged fluid increase with increasing initial liquid filling.
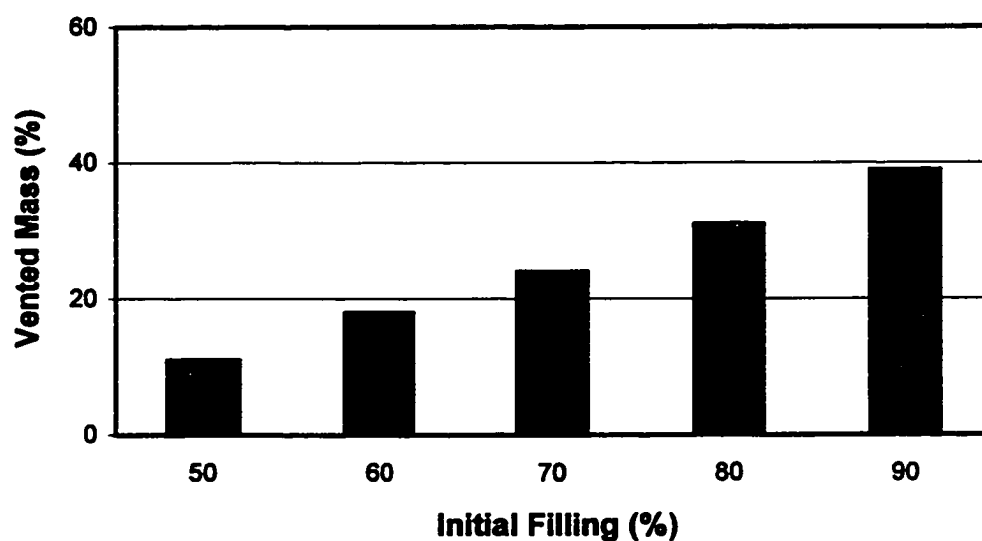

Figure 5 Effect of varying initial liquid filling on vented mass

The vessel pressure varies with time during depressurization. Three tests were performed with different initial liquid fillings of 50, 70, and 90% to predict the rate of pressure drop when venting SB/IA solution at an initial pressure of 80 psi. The resulting pressure-time profile is given in Figure 6.

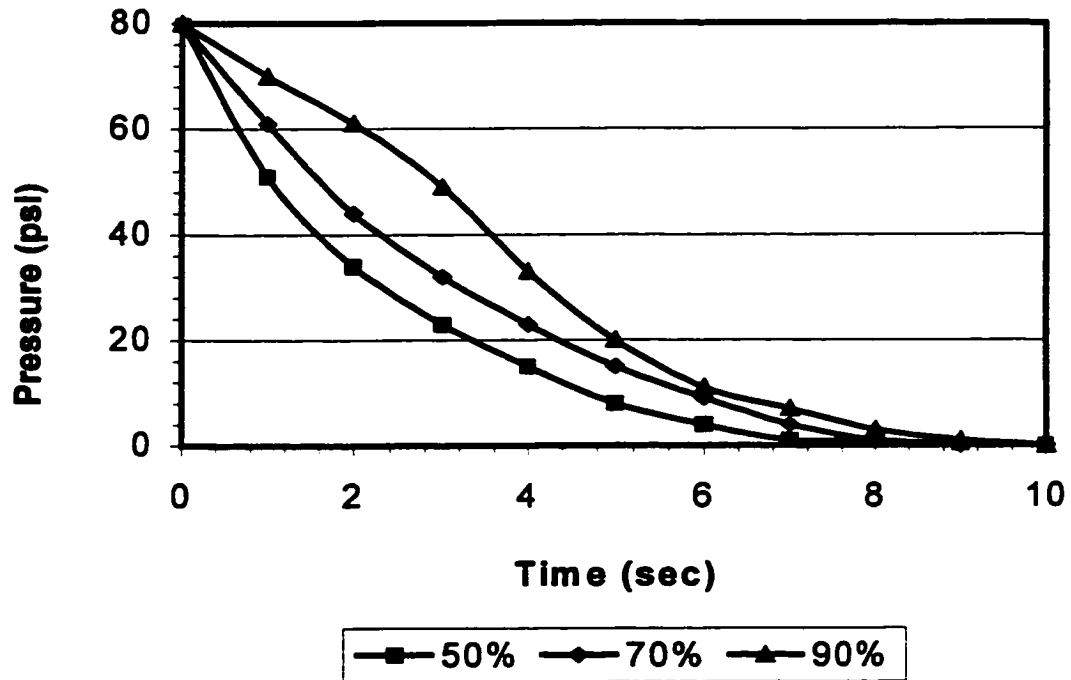Figure 6 Pressure-time profile for three different initial liquid fillings

Evidently, for the higher initial liquid level, the rate of pressure drop in the vessel is smaller (i.e., more delay is expected). The observed gradual decrease in the pressure drop can be explained by the fact that when the liquid phase comes into contact with the vessel top, vapor generated within the vessel is hindered from escaping through

the vent line. Thus the vapor pressure in the vessel rises momentarily, and it takes longer to vent.

4.2.2 Influence of Initial Pressure

A base case of 70% initial filling was used to determine the influence of initial pressure on the depressurization of SB/IA solution. The initial pressures chosen were 60, 80, 100 and 120 psi. A summary of test conditions is given in Table 2. The overall vented masses are presented in Figure 7 as a volume percentage of the initial mass inventory.

It can be concluded that the vented mass increases with increasing initial pressure. The vented mass is a combination of both the vapor formed due to flashing and the liquid entrained in the discharged flow. Thus, the liquid mass flow rate out of the vessel is directly proportional to the initial vessel pressure.

Table 2 Starting conditions for the initial pressure effect on vented mass

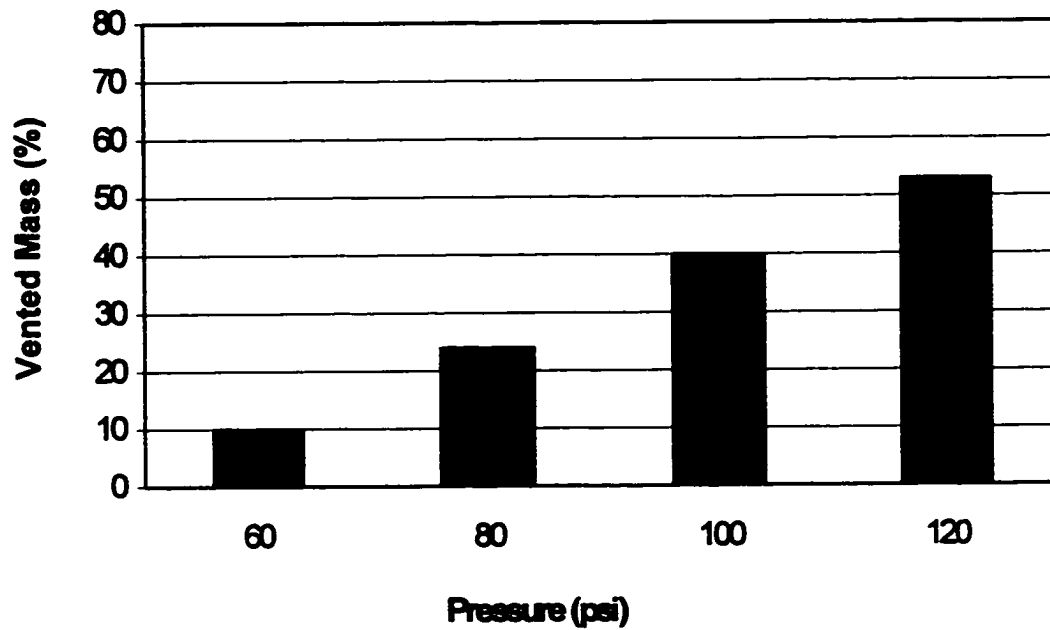| Test Fluid	SB/IA
Initial Pressure	60, 80,100, 120 psi
Initial Filling	70%
Viscosity	1 mPa.s
Vent Diameter	6.35 mm

Figure 7 Effect of varying initial pressure on the vented mass

The pressure-time profile inside the vessel during the depressurization of SB/IA fluids under initial pressure of 60, 80, and 100 psi is shown in Figure 8. Test conditions are summarized in Table 3.

Table 3 Starting conditions for the pressure-time profile of three different initial pressures

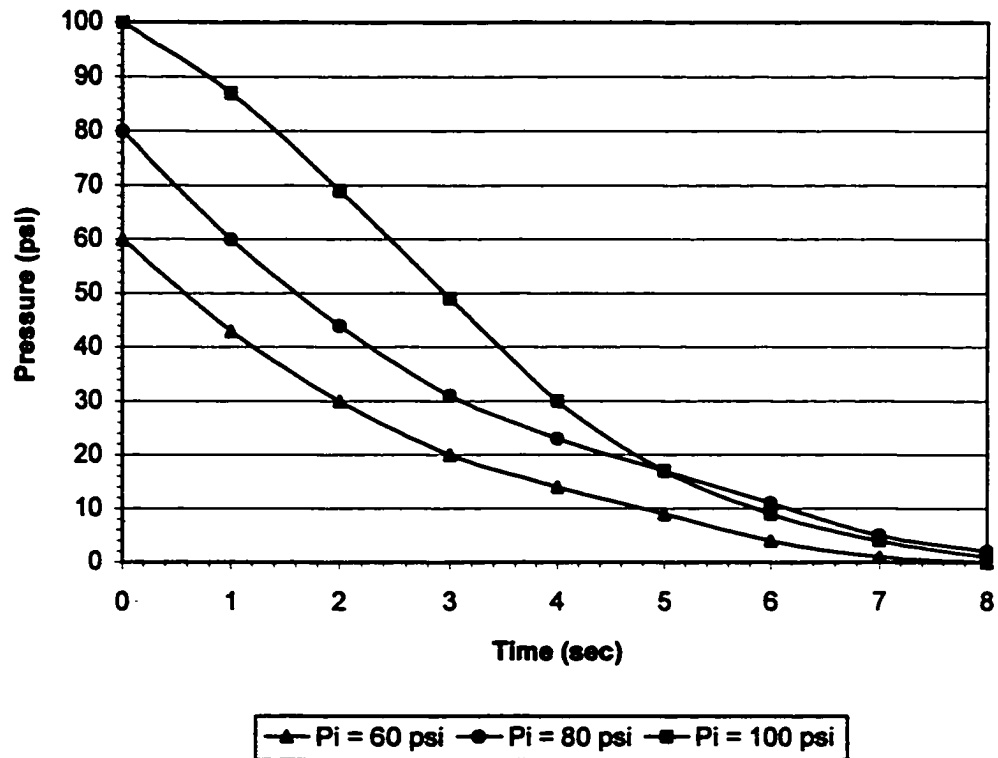| Test Fluid	SB/IA
Initial Pressure	60, 80, 100 psi
Initial Filling	70%
Viscosity	1 mPa.s
Vent Diameter	6.35 mm

Figure 8 Pressure-time profile for three different initial pressures

By examining Figure 8, one can conclude that the rate of pressure drop in the vessel increases with increasing initial pressures (i.e., for a higher initial pressure, the rate of pressure drop is smaller). This result might be attributed to the fact that more bubbles are generated with higher initial pressures and in agreement with the findings of Friedel and Purps [1984].

Interestingly, by studying the pressure-time profile, it was noticed that an initial pressure drop followed by a pressure rise characterizes the pressure profile at the early stages of the depressurization tests. During the initial moments of venting, the pressure drops sharply because of a delay in the start of bubble generation in response

to the pressure drop in the vessel. The system soon recovers due to the gas bubble generation throughout the bulk of the liquid. Then, due to vapor venting, the pressure starts gradually decreases again. This delay is very short and of fairly little impact on the system behavior and design. Thus, it will be excluded in our study.

Pressure fluctuation has been also observed during the depressurization tests. The oscillations exist in the pressure profile charts support such notice. Bell I. [1994] reported the same phenomenon. This result can be attributed to the venting of predominantly liquid mixture (when the vessel has large liquid content). Smooth pressure-time profile was noticed with the venting of predominantly vapor mixture (i.e., small liquid entrainment).

4.2.3 Influence of Vent Line Diameter

Two comparison tests were performed under the same initial conditions (80-psi pressure and 70% liquid filling) to study the depressurization behavior through two different vent lines. The two vent lines were the original vent line (6.35-mm) that has been used in section 4.2.1 and section 4.2.2 and 4-mm diameter vent with equal length. Table 4 summarizes the starting test conditions.

Figure 9 shows the dependence of the depressurization process on the size the vent line installed. As can be seen, the larger the vents line diameter, the larger the amount of vented mass. The vented mass was substantially decreased by 20% as a result of decreasing the vent line diameter size from 6.35mm to 4mm. In conclusion, the vented mass flux decreases due to a decrease in the vent line diameter.

Table 4 Starting conditions for the vent size effect on vented mass

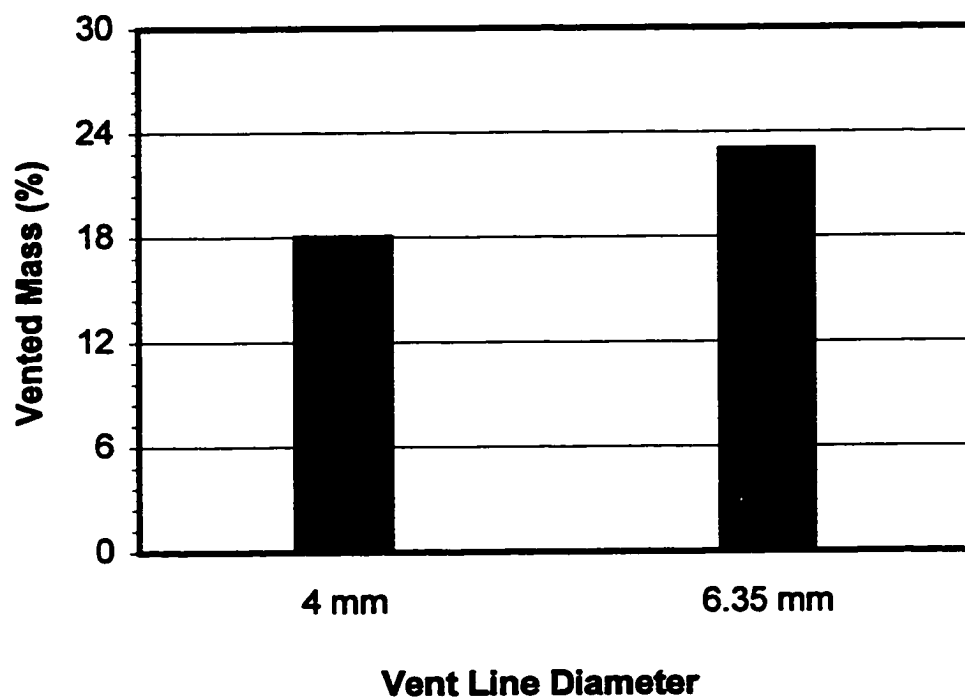| Test Fluid	SB/IA
Initial Pressure	80psi
Initial Filling	70%
Viscosity	1 mPa.s
Vent Diameter	4 and 6.35 mm

Figure 9 Effect of vent line size on the total vented masses

The pressure-time history in the vessel for the two vent lines has been given in Figure 10. The plot shows that the larger the vent line diameter, the higher the declining rate of pressure becomes (i.e., the vessel pressure falls more rapidly).

This phenomenon can be explained as follows: for the larger vent line, more vapor was vented within time of depressurization due to the greater quantity of bubbles passing through the vent line.
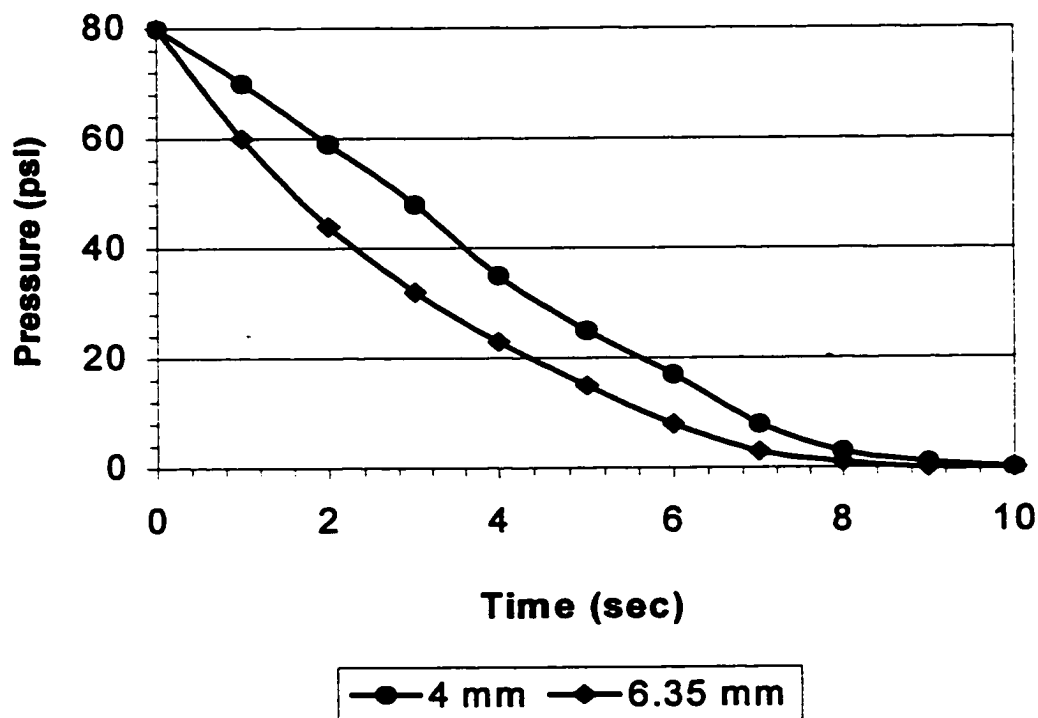

Figure 10 Pressure-time profile for the two vent lines

4.3 Results for High-Viscosity Fluids

High-viscosity fluids used in these tests were made by using CMC powder as described in section 3.3.2. Comparison tests were carried out using five different fluid viscosities in order to examine the viscosity effect on venting behavior. Viscosities

were measured as 10, 15, 22, 40 and 62 mPa.s. In all tests the initial pressure was held constant at 80 psi and the initial liquid filling was set at 70%. Test conditions are summarized in Table 5.

Table 5 Starting conditions for the effect of viscosity on the vented mass

Test Fluid	Viscous SB/IA
Initial Pressure	80psi
Initial Filling	70%
Viscosity	1, 10, 15, 22, 40, 62 mPa.s
Vent Diameter	6.35 mm

The overall vented mass is given in Figure 11 as a function of the liquid viscosity. The vented mass decreases as the liquid viscosity increases. A 5% increase in vented mass occurred in a vessel due to a change in viscosity from 1 mPa.s to 10 mPa.s. Upon opening the valve, small and homogenous bubbles are formed moving with low-rise velocity due to the liquid's high viscosity. The slower-moving bubbles having a relatively high residence time in the liquid bulk contributed more to the overall void fraction. Thus, the liquid level is kept higher and for longer times ensuring more two-phase venting. Through coalescence of small bubbles, large bubbles are formed which in contrast to the small bubbles move with a faster velocity through the liquid.
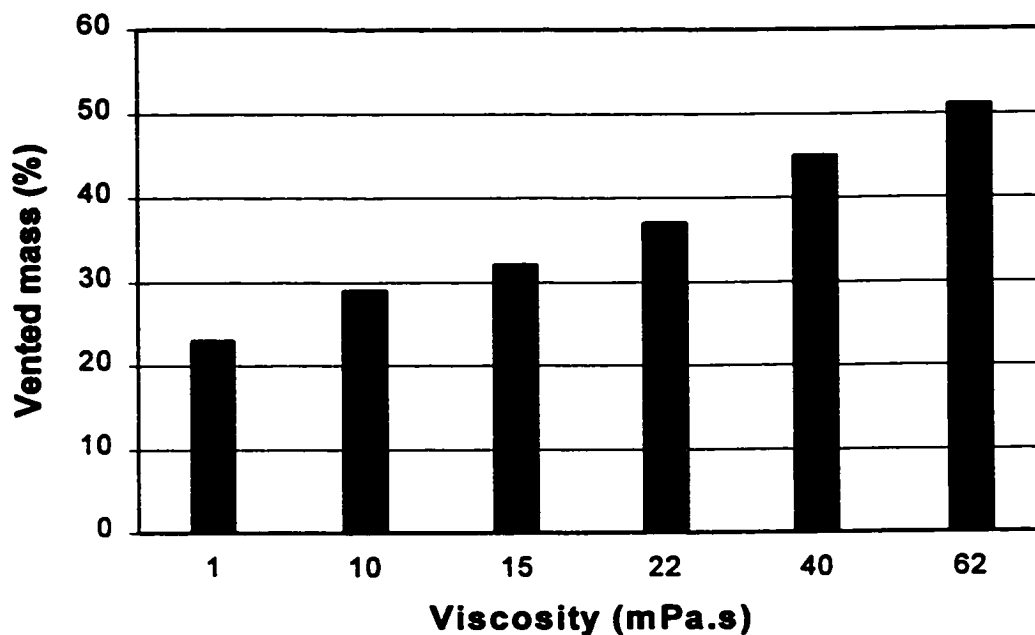
Figure 11 Effect of viscosity on vented mass

The vessel pressure-time profile during depressurization is presented in Figure 12. The results confirm that a significant difference in the flow pattern exists between the high- and the low-viscosity fluids. The rate of pressure decrease is much less in the high viscosity fluids.
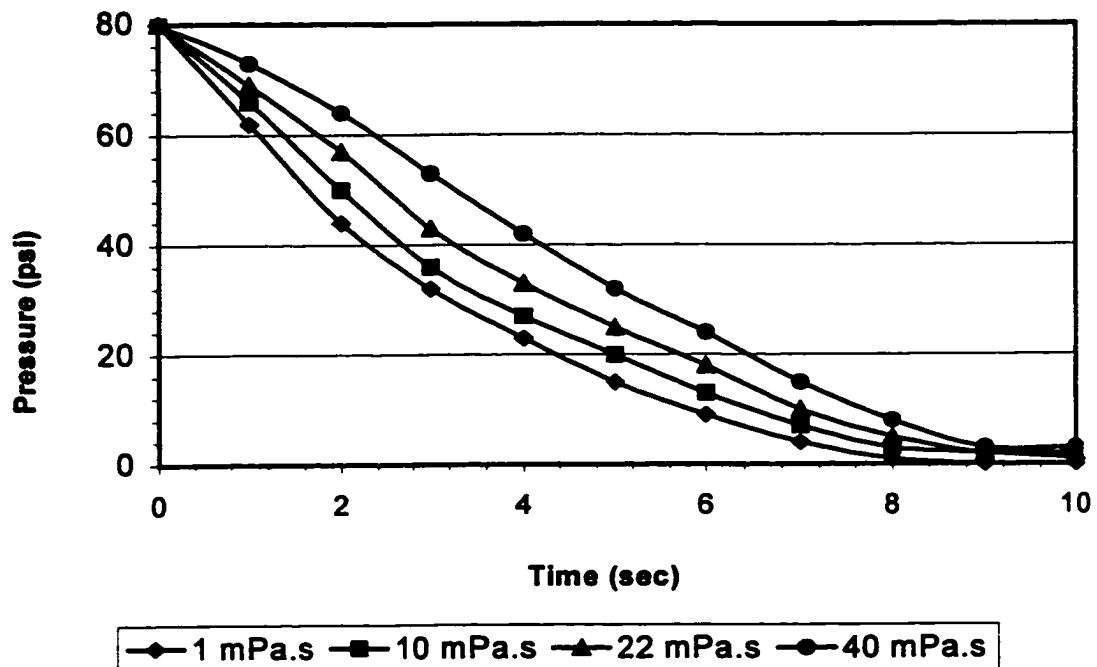
Figure 12 Pressure-time profile for different viscosity fluids

4.4 Results for Foamy Fluids

Two comparative tests have been carried out. One depressurization test was performed for SB/IA solutions with an initial liquid filling of 70% and an initial pressure of 80 psi. The other test was performed with the same initial conditions as the previous test but with the addition of 409-formula detergent to the water in the ratio of 1:200 by volume. The addition of 409-formula detergent causes water to foam, as described in section 3.3.3. Table 7 summarizes the test conditions.

Table 6 Starting conditions for the vented mass test of foamy solution

Test Fluid	Foamy SB/IA
Initial Pressure	80 psi
Initial Filling	70 %
Viscosity	1 mPa.s
Vent Diameter	6.35 mm

A comparison between the two fluids has been done on the bases of the overall vented masses. Figure 13 shows the vented masses as a percentage of the initial masses for the two cases. The foamy solution showed a greater vented mass, nearly three times the mass vented of the foam-less solution.
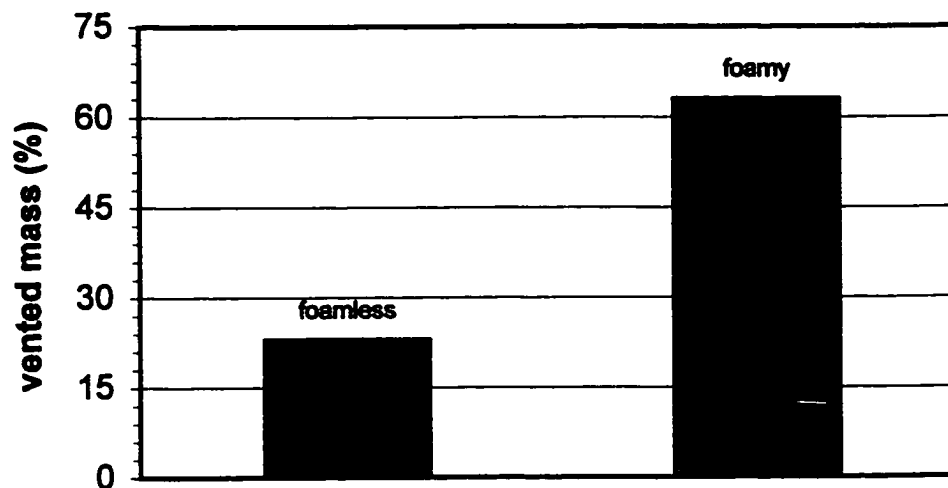
Figure 13 Vented masses for foam-less and foamy fluids

The pressure-time profile for the two cases is shown in Figure 14. If the two cases are compared, a difference in the venting characteristics can be seen. The foamy fluid shows a longer depressurization time and a slower rate of pressure drop. Because the rate of foam generation is larger the rate of discharge, the foam particles settled on the top of the liquid surface and filled the whole space above the liquid surface. Thus, the foam approaches the vessel top for a longer time, ensuring a longer two-phase flow venting.
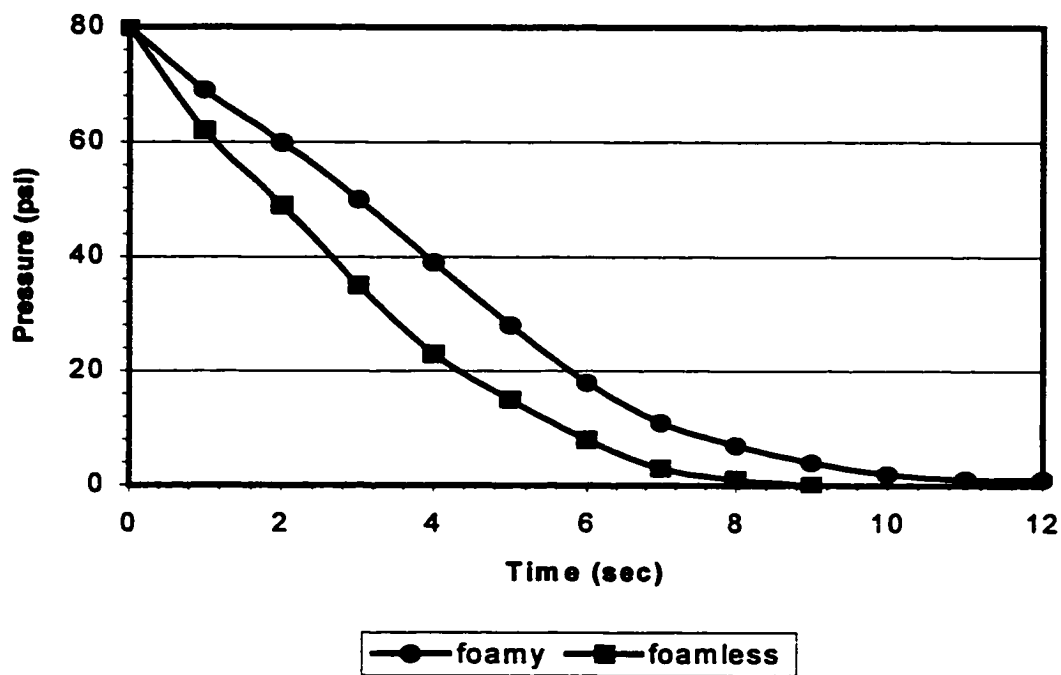
Figure 14 Pressure-time profile for foamy and foam-less fluid

Figure 15 show the initial liquid filling effect on the vented mass of foamy

SB/IA solution. The initial liquid filling shows a weak effect on venting mass of foamy

solutions. Comparison between the initial filling effect on the total vented mass for

foamy and foam-less solutions (under same starting conditions of pressure and initial

filling) is given in Figure 15. For foamy solutions, only 6% increase in the vented mass

resulted from a 40% increase in the initial liquid filling, compared with 28% for the
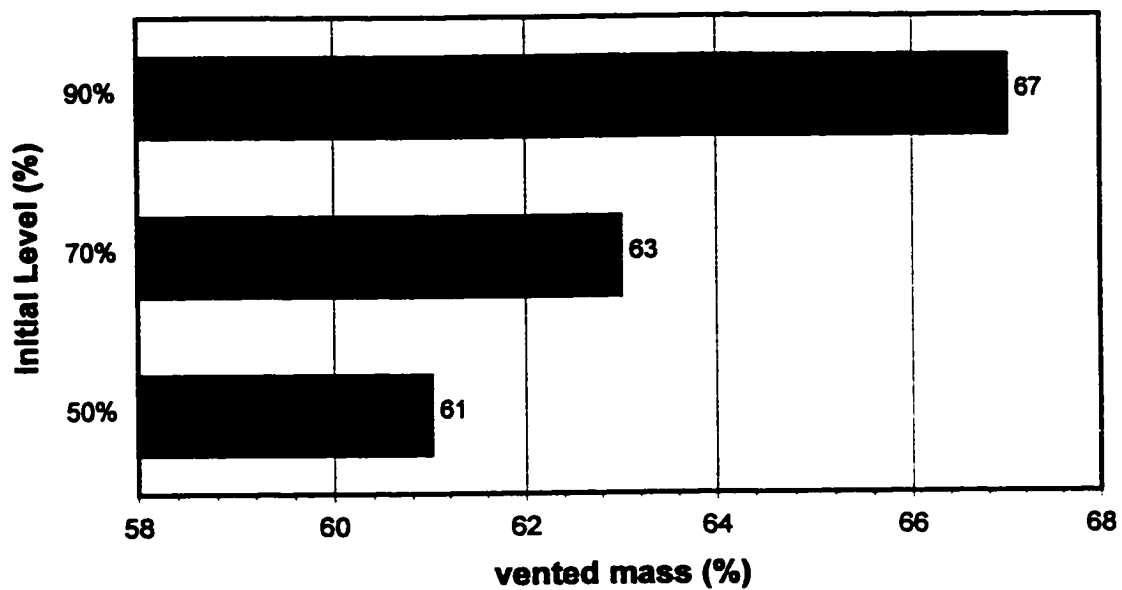
foam-less solution.

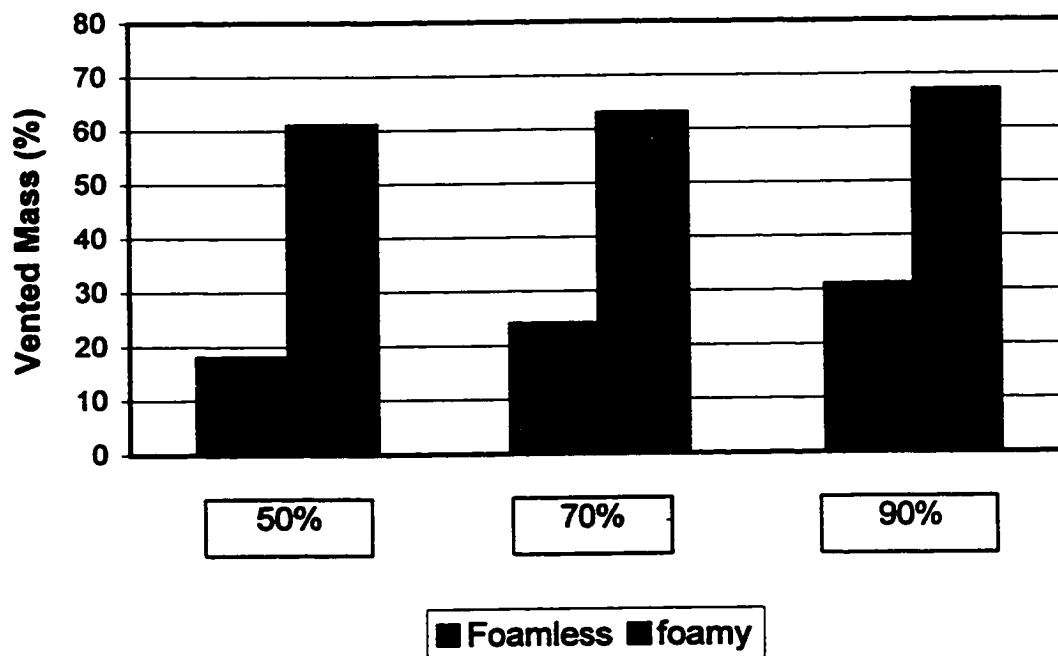Figure 15 Effect of varying initial liquid filling on the vented mass of foamy fluid

Figure 16 Comparison between varying the initial filling on vented mass for foamy and foam-less fluids

The behavior of different fluids during depressurization helps to understand the venting characteristics and the associated flow patterns. The vented mass as a ratio of the initial mass inventory is given in Figure 16 for three types of fluid. Foamy and foam-less SB/IA solutions and high-viscosity SB/IA solution were compared on the basis of the total vented mass under same initial conditions of 80 psi pressure and 70% initial liquid filling. The foamy solution exhibited the largest amount of vented mass. The foam-less solution produced the smallest amount of vented mass due to the fast depressurization of the vapor phase with low amount of liquid entrainment. The above results are in line with the findings of Bell [1994].

It has been noticed that the rapid depressurization of both foamy and viscous fluids resulted in the immediate appearance of bubble cloud in the bulk of the liquid (emulsion). Bubbles formation takes place through out the volume of the liquid. Bubbles displace the liquid surface upward toward the vent causing two-phase flow.
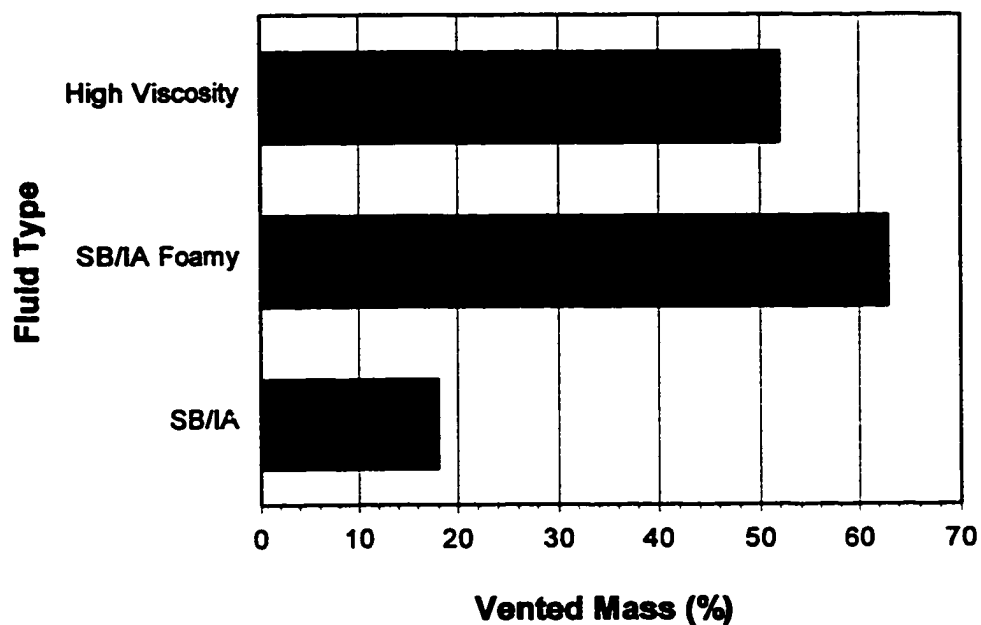
Figure 17 Comparison between the vented mass for different fluid types

The pressure-time history in the vessel for the previous three types of fluids at the same starting conditions is given in Figure 18. For the viscous and foamy fluids, a longer two-phase depressurization time (hindering the release of more vapor) causes the small rate of pressure drop compared to the foam-less solution.
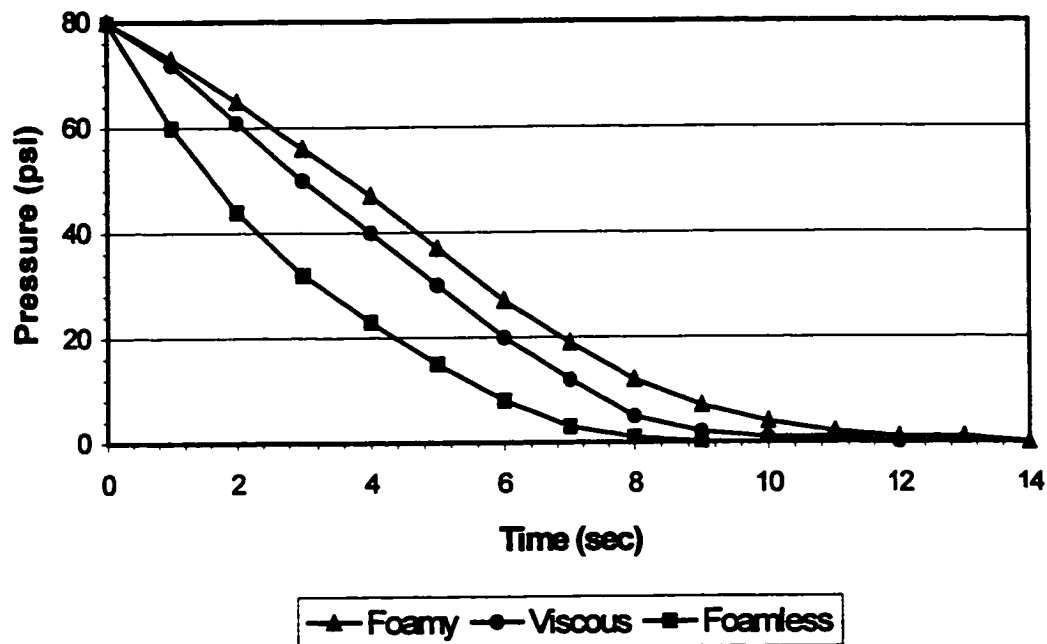
Figure 18 Comparison between the pressure-time profile of different fluid types

For the three types of fluid, the pressure time history is in proportion with the vented mass exhibited in Figure 17 (i.e., the foamy solution vented the largest mass and shows the lowest rate of pressure drop followed by the viscous solution then the foamless solution). The viscous fluid showed less vented mass compared to the foamy fluid due to the presence of the large bubbles which caused higher rate of pressure drop by removing more vapor while leaving the vessel.

It is clear that the high-viscosity fluid is similar to the foamy in terms of the pressure profile and the overall time of depressurization. However, vented mass is different.

4.5 Bubble Characteristics

A series of depressurization tests were carried out with different initial conditions of liquid filling, vessel pressure, and working fluid properties. Description of the resulting bubble characteristics for each case is detailed below, based on the high-speed, digital camera recordings.

Rising bubbles in a swarm are not of fixed shape and size; for this reason, only velocity and shape of individual bubbles are accounted for in the present study. A scale tape was placed at the vessel wall to serve as a basis for image dimensions. Figure 19 shows an image of some bubbles taken by the HCCD camera. It is worthy to note that throughout the following discussion, bubbles are considered spherical in shape unless otherwise noted.
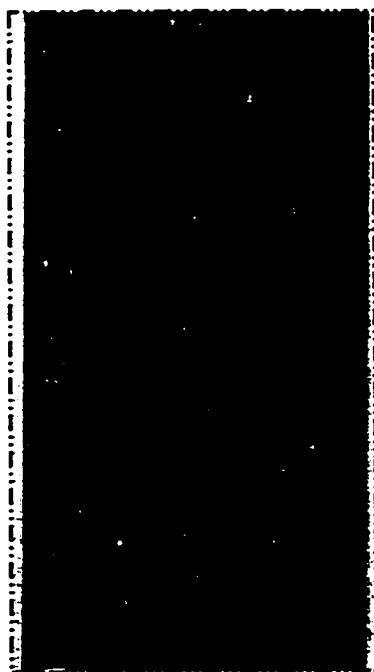
Figure 19 Bubbles image taken by the high-speed, digital camera

4.5.1 Bubble Shape

In this study, we will use the general practice of characterizing the bubble shape by using the so-called bubble aspect ratio "E", defined as the ratio of the bubble horizontal diameter d_h to the vertical length d_v as shown in Figure 20.
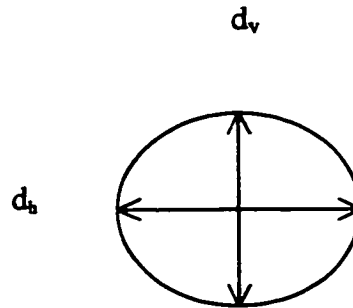
Figure 20 Definition of the bubble aspect ratio

For example, bubbles are considered spherical if they are symmetrical around the horizontal and vertical axis (i.e., aspect ratio close or equals 1). Enlarged images were made possible using the V for window software. The enlarged images were about 2-6 times the actual size.

Based on the photographic observation, bubbles up to 1.5-mm diameter are spherical. Few large bubbles are seen in the liquid with a cap shape. Figure 21 shows some enlarged bubble images of sperical shape.

Spherical bubbles were observed over the whole range of fluid viscosities given in section 4.3. A homogeneous two-phase bubbly flow pattern was observed for the foam-less solutions, where small spherical bubbles are distributed over the whole volume of the liquid.
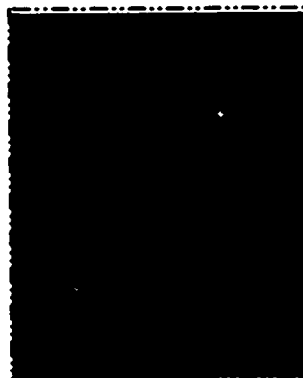
Figure 21 Spherical shape bubble image

4.5.2 Bubble Size

Bubble size was measured by examining images (with a known magnification) of individual bubbles photographed by the high-speed, digital camera. Bubble dimensions are recorded by reading the number of pixels, which represents the length and the width of a bubble. It was possible to roughly determine the average bubble size of a representative sample of 10 bubbles picked up from the images. Figure 22 shows two images of different bubble sizes.

Figure 22 Images of different bubble sizes

4.5.2.1 Foam-less fluid. bubbles of approximately 1.4-mm size were observed during the depressurization of SB/IA solution under pressure of 80 psi and initial level of 70%.

4.5.2.2 Foamy fluid. For foamy fluids, the measured bubble size was smaller compared to the non-foamy fluids. An average size of 0.9-mm was obtained for the foamy fluids compared to 1.4-mm for foam-less fluid under the same initial conditions. Nearly a 35% decrease in the bubble size occurred due to the foamy nature (resulted from the addition of the surface-active detergent). The bubble size reduction can be attributed to the working fluid lower surface tension. The bubble rises through the liquid on the form of swarms or clouds, not as individual bubbles. It has been also noticed that foam particles of same size settled on (before collapsing) the fluid surface at the end of the depressurization test.

4.5.2.3 Pressure effect. Comparison between the bubble size of SB/IA solutions operated under three different pressures of 80, 100, and 120 psi was made. Selected photographs of generated bubbles are enlarged to compare the bubble size. As a result, smaller bubbles were formed for fluids under higher pressure. A small number of large bubbles with a large rise velocity were frequently observed at low pressures.

4.5.2.4 Viscosity effect. For high viscosity fluids, tiny small bubbles have been noticed. The bubbles travel very slowly in the liquid bulk (they appear to be stagnant) thus, contributing more to the vessel void fraction. Table 7 shows the bubble size for six different viscosity fluids. The bubble size was found using bubble images obtained by the high-speed camera. Images were taken under constant pressure of 80 psi as

described in section 3.4.2. The bubbles are showing tendency to increase in size with increasing the fluid viscosity.

Table 7 Effect of varying fluid viscosity on bubble size

Viscosity (mPa.s)	10	15	22	40	62
Bubble Size (mm)	0.5	0.55	0.75	0.8	1

4.5.3 Bubble Rise Velocity

In section 2.7 it was noted that in order to model the bubble hold-up in a liquid knowledge of the bubble rise velocity is needed. By examining a time-series photographs of bubbles, one can make measurements of the bubble rise velocity. The distance traveled by a bubble between two consecutive frames can be analytically measured by counting the number of pixels. A pixel is a picture element that contains a single charge packet. For the camera in use (Quantix), each pixel is 20-48 micrometer square as shown in Figure 23.
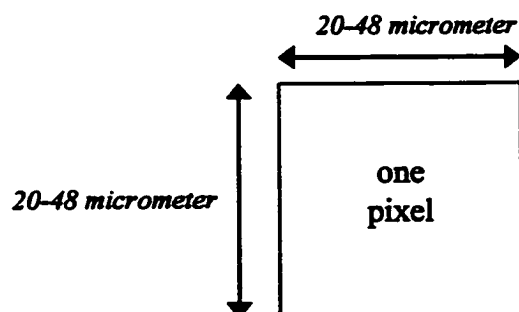
Figure 23 Pixel dimensions

Four time-sereies bubble images taken at a fixed rate of 20 frames per second are shown in Figure 24. The selected bubble images are photographed by the high-speed camera for 15 mPa.s SB/IA solution. Tracking the movement of the circled bubble (picked as an example from Figure 24) shows a travel distance of 2.4 cm in 200 msec time, corresponding to a rise velocity of 8 cm/sec. It was noticed that bubbles rise freely as individual bubbles without any interference from neighboring bubbles. However, for foamy fluids bubbles rise as a dense swarm.

Figure 24 Time series photographs

4.5.3.1 Bubble size effect. An increase in the bubble size is expected to increase the buoyancy force, and hence the bubbles' rise velocity increases. Smaller bubbles were noticed rising slowly through the liquid bulk compared to larger bub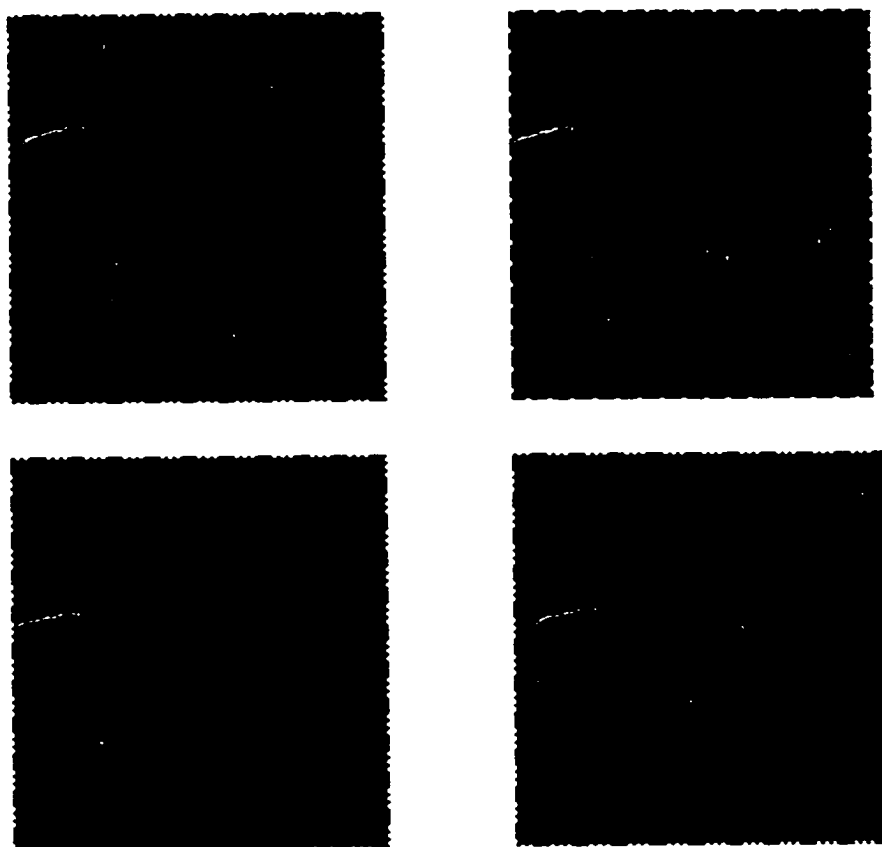bles. For example, the rise velocity of a 1-1.5mm-diameter bubble was nearly half the rise velocity for bubbles with a diameter of 1.5-3mm.

4.5.3.2 Viscosity effect. Table 8 shows the estimated bubble rise velocity for SB/IA solution with different viscosities. Higher viscosity makes the bubbles harder to moveand consequently reduces the bubble rise velocity. It can be concluded that the rise velocity decrease due to an increase in the working fluid viscosity.

Table 8 Effect of varying fluid viscosity on the bubble rise velocity

Viscosity (mPa.s)	1	10	15	22	40	62
Bubble Rise Velocity (cm/sec)	14	10	5.6	5.2	4.6	3.5

CHAPTER 5

CONCLUSIONS AND RECOMMENDATIONS

5.1 Conclusions

Experiments have been carried out for top venting of saturated fluids. Differences in the venting characteristics for a range of fluid systems (viscous, foamy, and foam-less) have been attributed to the flow pattern inside the vessel. Key issues and physical phenomena governing the depressurization have been discussed.

In conclusion, this study has added basic information on the two-phase fluid behavior. Based on the experimental results for the depressurization of saturated fluids and the subsequent discussion and analysis, the following conclusions are offered:

1. Various test fluids having been investigated,

   - Water produced the fastest depressurization rate with the least amount of swell level and the least amount of two-phase flow venting.

   - Foamy fluid produced the slowest depressurization rate and the longest two-phase flow venting.

   - The viscous fluid showed a vented mass of value between the foam-less and the foamy fluids.

61

2. The depressurization phenomenon was strongly dependent on various influential parameters, namely the initial liquid filling and the initial pressure. Both foamy and foam-less fluids showed an increase in the vented mass and the depressurization time in response to an increase in the initial liquid filling. However, the foamy fluid showed a weak dependence on the initial liquid filling.

4. Fluid viscosity was found to have a substantial effect on the rate of pressure drop and the overall vented mass. Increasing the viscosity slows down the depressurization and increases the vented mass.

5. Venting of foamy fluids is characterized by

- A much slower rate of depressurization; it takes longer to vent a foamy fluid compared to non-foamy and viscous fluids.

- Higher vented mass compared to both the foam-less and the viscous fluids.

- Longer two-phase flow over the depressurization period.

6. Vent line diameter has been found to influence the depressurization behavior. Smaller vent line gives lower bubble generation resulting in less vented mass and slower depressurization.

7. Bubble characteristics are studied under different starting conditions. It was concluded that

- Bubble shape was found to be spherical over most of the experiment range.

- The foamy nature of the fluid produced a smaller bubble size (40% reduction).

- Increasing the vessel initial pressure decreases the produced bubble size.

- The bubble size and the fluid viscosity influenced bubble rise velocity. Bubble rise velocity significantly decreases as one or both of the above variables increase.

8. Vessel flow pattern of high-viscosity and foamy fluids was characterized by the presence of very small bubbles forming two-phase emulsion through which large bubbles are moving upward. The vessel contents behave as homogeneous two-phase mixture.

9. Although the current study was conducted with certain type of fluids, the general approach appears to be compatible with other fluid analysis. The results can be used as a screening tool to test the potential for two-phase vent flow. Published data of previous investigations were found comparable with the current findings.

5.2 Recommendations

The experimental results described in chapter 4 illustrated several interesting conclusions. However, in light of our findings, much work remains to be accomplished in the area of depressurization of two-phase flow. The following are some recommendations for future work.

- Further experimental studies would be of value covering a wider range of vessel pressure, fluid viscosity, and surface-active agents.

- The results that have been obtained should be examined and compared to full- scale depressurization studies. Further information on the bubble growth mechanism is needed to resolve the question of the distribution of the two phases relative to each other.

- The results and the corresponding analysis have been determined only for the current experimental starting conditions. However, the obtained experimental results may permit certain conclusions about large–scale systems. Attempts can be made to orient the results toward full-scale depressurization system by determining the scale-up parameters required in extrapolating the results to a larger scale relevant to the chemical industry.

- Further work can be done to investigate the effect of the blow down valve location. Namely, the bottom blow-down configuration tests. Also, work can be done to repeat the current analysis for a horizontal vessel.

- A mathematical model for the formation of the two-phase emulsion (for the foamy and high-viscosity fluids) would be of great use.

5.3 Error Analysis

Usually, error analysis gives some indications and assurances as to the accuracy and reliability of the study.

External and internal estimates of errors are involved in the present study. External errors are based on the general conditions of experimental test facility. The internal errors are based on the obtained experimental results.

Other type of errors included personal errors and mistakes that occurred during the experiment, but through proper design of the experimental procedure this type of error was reduced. It is reasonable to assume the reproducibility of the results because the average of two or three runs was taken for each test.

APPENDIX A

THE QUANTIX HCCD CAMERA

The high-resolution Charge Coupled Device (CCD) cameras have allowed the traditional film-based method to be replaced. A multiple CCD array arrangement allows two or more CCD arrays to look through the same set of imaging optics. The resulting image processing is totally digitized. The high frame rate gives the possibility of measuring time dependent flows and accelerations. Other benefits include standardized connectors and software for interpreting and analyzing the images.

Quantix Delivers:

- Low-noise, high-speed camera operation.

- Compact one-piece design.

- 12 bits at 1 million or 5 million pixels per second readout rate.

- Cooled CCD (-25°C forced air, -35°C liquid circulation).

- C- or F-mount option with an integrated, high-speed shutter.

- TTL interface to coordinate with other equipment.

- PCI, ISA, or SCSI to support PC, Macintosh, Sun, or Silicon Graphics platforms.

65

Multiple Detection Modes

Quantix operates in three distinct detection modes (gain settings) to address varying requirements:

- High Sensitivity to detect weak signals.

- High Dynamic Range to measure bright and dim signals within the same image at full spatial resolution.

- High Signal-to-Noise Ratio to distinguish a faint signal on a bright background for photon noise-limited experiments.

APPENDIX B

CARBON DIOXIDE DATA

For carbon dioxide at 0 ^{0}C, 1 atm;

- Density: 1.98 g/l, or 0.123 lb/ft^3.

- Boiling Point: -76.5 ^{0}C

- Solubility: 197.9 cm^3 in 100-gram water.

Quinn [1945] reviewed the solubility of carbon dioxide in various solvents; alcohol solubility data expressed in terms of the Ostwald solubility coefficient (L) are given in Table 9. Ostwald solubility coefficient is defined as the ratio of the gas in the liquid phase to its concentration in the gas phase.

One of the most useful units to express the solubility of a gas is the Bunsen Absorption Coefficient ($\propto$). It is defined as the ratio of the gas volume passes into solution through unit area in unit time to the volume of the gas, which is similarly, passes out of solution. Quinn [1945] also reported a good review for the solubility of carbon dioxide in organic compounds. Table 10 lists some selected data.

Table 9 Solubility of carbon dioxide in certain organic solvents at 25 ^{0}C.

SOLVENT	SOLUBILITY COEFFICIENT (L)
Water	0.8256
Toluene	2.305
Benzene	2.425
Propyl Alcohol	2.498
Ethyl Alcohol	2.706
Methyl Alcohol	3.837
Acetic Acid	4.679
Acetone	6.295
Methyl Acetate	6.494

Table 10 Solubility of carbon dioxide in solutions of organic compounds at 15.5 ^{0}C.

COMPOUND	MOLES OF COMPOUND PER LITER SOLUTION	ABSORPTION COEFFICIENT α
$Na_4B_4O_7$	0.25	5.741
$NaBO_2$	0.25	5.478
$Na_3PO_4.12H_2O$	1.0	3.932
$Na_4P_2O_7.10H_2O$	1.0	5.709
KBr	1.0	0.863
KI	1.0	0.710

BIBLIOGRAPHY

Adamson A., *Physical Chemistry of surfaces*, Wiley Interscience Publication, 4th edition, NY, (1982).

Akita K., and Yoshida F., "Bubble size, interfacial area, and liquid-phase mass transfer coefficient in bubble columns," *Ind. Eng. Chem., Process Des. Develop.*, Vol. 13, No. 1, pp. 84-88, (1974).

Allan R., Charles G., and Mason S., *Journal of Colloid Science*, Vol. 16, pp. 150-165, (1961).

Amon M., and Denson C., "A study of the dynamics of foam growth; Analysis of the growth of closely spaced spherical bubbles," *Poly. Eng. Sci.*, Vol. 24, No 13, pp. 1026, (1984).

Attar A., "Bubble nucleation in viscous material due to gas formation by a chemical reaction: Application to coal pyrolysis," *AIChE Journal*, Vol. 24, No. 1, pp. 1106-115, (1978).

Bell I., *Top venting of low and high viscosity fluids during vessel depressurization* University Degree Thesis, University of London, (1994).

Bell I., Morris S., and Oster R., "Vent line void fractions and mass flow rates during top venting of high viscosity fluids," *J. Loss Prev. and Process Ind.*, Vol. 6, No 1, (1993).

Bell I., and Morris S., "Flow visualization during top venting from a small vessel," *J. Loss Prev. Process Ind.*, Vol. 5, No 3, pp. 160-164, (1992).

Blander M., and Katz J., "Bubble nucleation in liquids," *AIChE Journal*, Vol. 21, No. 5, pp. 833, (1975).

Boesmans B., and Berghmans J., "Axial void fraction distribution effects on level swell during emergency pressure relief," *J. Loss. Prev. Process Ind.*, Vol.8, No. 1, pp. 3-10, (1995).

Boyle W., *Chemical Engineering Progress*, Vol. 63, No.8, pp. 61 (1967).

Cole R., "Boiling nucleation," *Advancement in Heat Transfer*, Vol. 10, pp. 85, (1974).

Dongming L., "Coalescence between small bubbles: Effects of bulk and surface diffusion," *Chemical Engineering Science,* Vol. 51, No. 14, (1996).

Fan L., and Tsuchiya K., *Bubble wake dynamics in liquids and liquid-solid suspensions* Butterworth-Heinemann, Stoneham, MA, (1990).

Fauske H., et al., *Technology Report on Hydrodynamic Methods for Emergency Relief Systems,* DIERS Report FGH+T- DIERS-10, August (1981).

Fauski & Associates Inc., *Flashing viscous flow of polystyrene mixtures: Test data and scale-up methods,* Report No. FAI/89-26, Burr Ridge, IL, (1989).

Fauski H., *Relief system designs for runaway chemical reactions,* Proceedings of International Symposium, Preventing major chemical accidents, CCPS, Washington, D. C., February, (1987).

Fauski H., and Leung J., "New experimental technique for characterizing runaway chemical reactions," *Chemical Engineering Progress,* pp. 39-46, (1985).

Finke P., *Phase separation in viscous fluids,* University Degree Thesis, University of Munich, (1990).

Fisher H., "The DIERS users group: A forum for development/dissemination of emergency Relief system designs technology," *Plant/Operations Progress,* Vol. 8, No. 2, pp. 70-72, (1989).

Fisher H., "An overview of emergency relief system design practice," *Plant/Operations Progress,* Vol. 10, No. 1, pp. 1-12, (1991).

Fisher H., *Emergency relief system design using DIERS technology,* DIERS project manual, AIChE publication, (1992).

Friedel L., and Purps S., "Phase distribution in vessels during depressurization," *The Int. J. of Heat and Fluid Flow,* Vol. 5, No 4, pp. 229-234, (1984).

Griffith, P., and Wallis D., "The role of surface conditions in nucleate boiling," *Chemical Engineering Symposium Series,* Volume 56, No 30, (1960).

Grolmes M., Leung J., and Fauski H., "Large scale experiments of emergency relief systems," *Chemical Engineering Progress,* Vol. 81, No. 8, pp. 57-62, (1985).

Haberman W., and Morton R., *An experimental investigation of the drag and shape of air bubbles rising in various liquids,* Report No. 802, Navy Department, Washington, DC.

Hardy P., and Richter H., "Present transient and two-phase swelling due to a small top break," *Nuclear Engineering And Design*, Vol. 95, pp. 207-220, (1986).

Hetsroni, G., *Handbook of multiphase systems*, Hemispheres Publishing Corporation, (1982).

Huff J., "AIChE Tech. Manual," *Loss Prevention*, Vol. 7, pp. 45 (1973).

Idogawa K., Ikeda K., Fukuda T., and Morooka S., "Behavior of bubbles of air-water system in a column under high pressure," *Inter. Chem. Engineering*, Vol. 26, pp. 468, (1986).

Jiang J., Arters D., and Fan L-S., " Pressure effects on hydrodynamic behavior of gas-liquid-solid fluidized beds," *Ind. Engineering Chem. Research*, Vol. 31, pp. 2322, (1992).

Jiang P., Arters D., and Fan L-S., "Flow visualization of high-pressure (21 MPa) bubble column: Bubble characteristics" Transactions of the Institute of Chemical engineering, Vol. 73, Part A, (1995).

Kenrick F., Wismer k., and Wyatt k., "Supersaturation of gases in liquid," *The Journal of Physical Chemistry*, Vol. 28, (1924).

Marrucci G., "Rise velocity of a swarm of spherical bubbles," *I&EC Fundamentals*, Vol. 4, No. 2, pp. 224-225, (1965).

Mendelson H., "The prediction of bubble terminal velocities from wave theory," *AIChE Journal*, Vol. 13, No. 12, pp. 2150, (1967).

Morris S., Bell K., and Oster R., "Top-venting of flashing high-viscosity fluids," *Chemical Engineering and Processing*, Vol. 31, pp.297-305 (1992).

Natarajan M., *Principles of Fluid Mechanics*, Oxford & IBH Publishing Co., (1984).

Oster R., Bell K., and Kottowski, M., "Hydrodynamic considerations of venting with high viscosity non-reacting fluids," *J. Loss Prev. and Process Ind.*, Vol. 3, (1990).

Quinn E., and Jones C., *Carbon Dioxide*, Reinhold Publishing Corporation, NY, (1945).

Reilly I., Scott D., De Bruijn T., and Macintyre D., "The role of gas phase momentum in determining gas holdup and hydrodynamic flow regimes in bubble column operation," *Canadian Journal of Chemical Engineering*, Vol. 72, pp. 3, (1994).

Sagert N., and Quinn M., *Journal of Colloid Science*, Vol. 65, pp. 415-422, (1978).

Sheppard C., and Morries S., *Two phase flow disengagement prediction via drift flux correlations*, Joint Research Center, Institute for Safety Technology, Technical Note No. I.944.112, August (1994).

Skouloudis A., and Kottowski, H., *One-dimensional analysis of five depressurization cases for vessels with top or bottom vent lines*, Process Engineering Division, JRC, Ispra, Commission of the European Communities 21020, Ispra (VA), Italy, (1990).

Skouloudis, A., and Kottowski, H., *Hydrodynamic aspects of venting for vessels containing viscous fluids*, Process Engineering Division, JRC, Ispra, Commission of the European Communities 21020, Ispra (VA), Italy, (1991).

Street J., Fricke A., and Reiss L., "Dynamics of phase growth in viscous, non-Newtonian liquids," *Ind. Eng. Chem. Fundam.*, Vol. 10, No. 1, pp. 54, (1971).

Vassallo P., Symolon P., Moore W., and Trabold T., "Freon bubble rise measurements in a vertical rectangular duct," *Journal of Fluids Engineering*, Vol. 117, pp. 729-732, (1995).

Wallis G., *"One dimensional two-phase flow*, McGraw-Hill, (1969).

VITA

The author was born in Zarqa, Jordan, on October 26, 1964. He is the son of Mr. Husain Alramadneh and Mrs. Fathiah Alramadneh of Malka, Jordan. He received his primary and secondary education in Zarqa, Jordan, graduating from Moghirah High School in 1983. He joined the Jordan University of Science and Technology and graduated with a Bachelor of Science in Chemical Engineering in February 1989.

Mr. Alramadneh enrolled in the Graduate School of Louisiana Tech University in the fall of 1992 and graduated with a Masters of Science in Chemical Engineering in February of 1994. In September 1994 he enrolled again in the Graduate School of Louisiana Tech University in the pursuance of a Doctorate Degree under the direction of Dr. Charles Sheppard. During his stay at Louisiana Tech he served as a teaching assistant (September 1994-April 1998). After receiving his Doctorate, he plans to pursue a consulting career in the chemical engineering.

73

IMAGE EVALUATION
TEST TARGET (QA-3)

150mm

6"
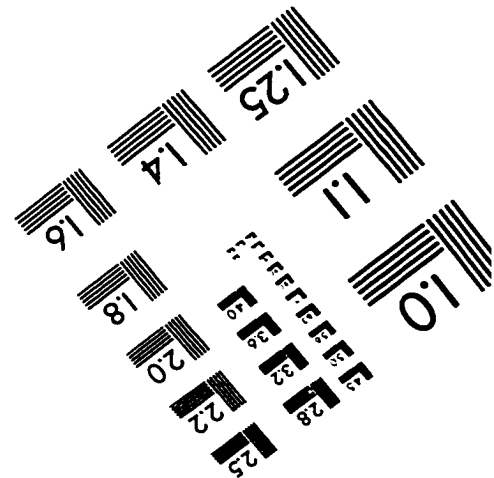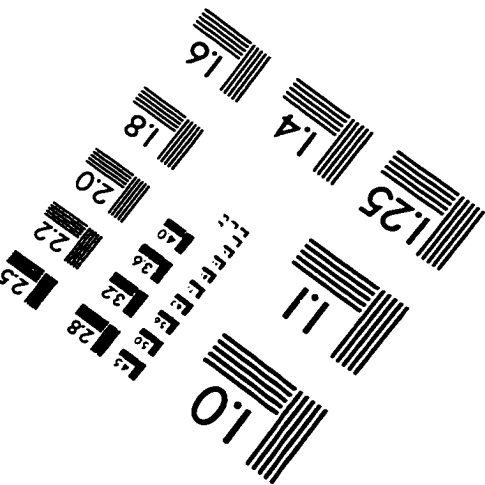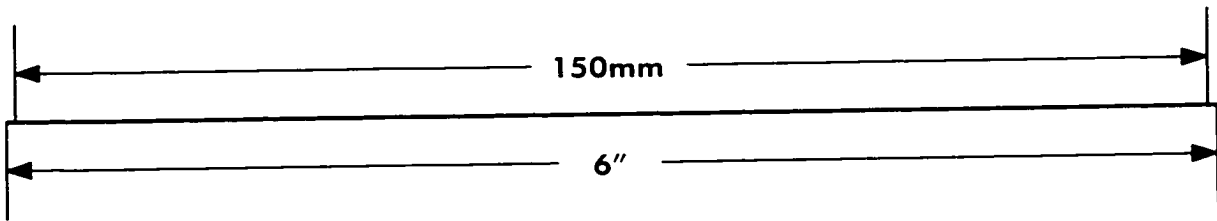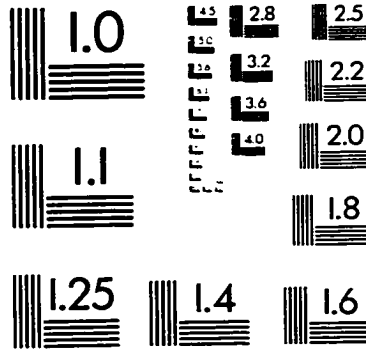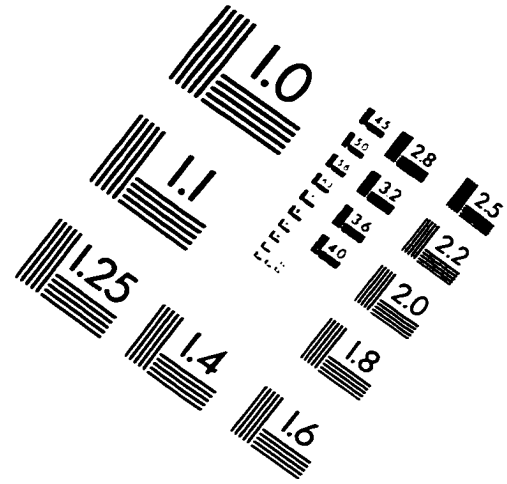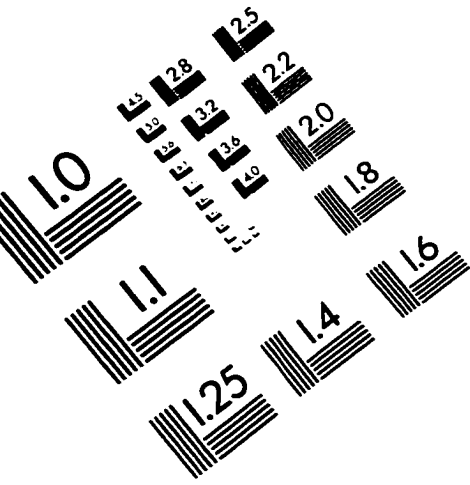
APPLIED ✦ IMAGE . Inc
1653 East Main Street
Rochester, NY 14609 USA
Phone: 716/482-0300
Fax: 716/288-5989